Di-leptons (mostly TCS) at the Electron-Ion Collider

Daria Sokhan
CEA Saclay

Prospects on various aspects of the dilepton probe in hadron physics
IJClab – Paris-Saclay - 25th November 2021

Electron-Ion Collider

World's first polarized electron-proton/light ion and electron-Nucleus collider.

For e-N collisions at the EIC:

- ✓ Polarized beams: e, p, d/^{3}He
- ✓ e beam 3 - 10 (18) GeV
- ✓ Luminosity L_{ep} ~ 10^{33-34} $cm^{-2}s^{-1}$
- ✓ 20 - 100 (140) GeV Variable CoM

For e-A collisions at the EIC:

- ✓ Wide range of nuclei
- ✓ Luminosity per nucleon same as e-p
- ✓ Variable centre of mass energy

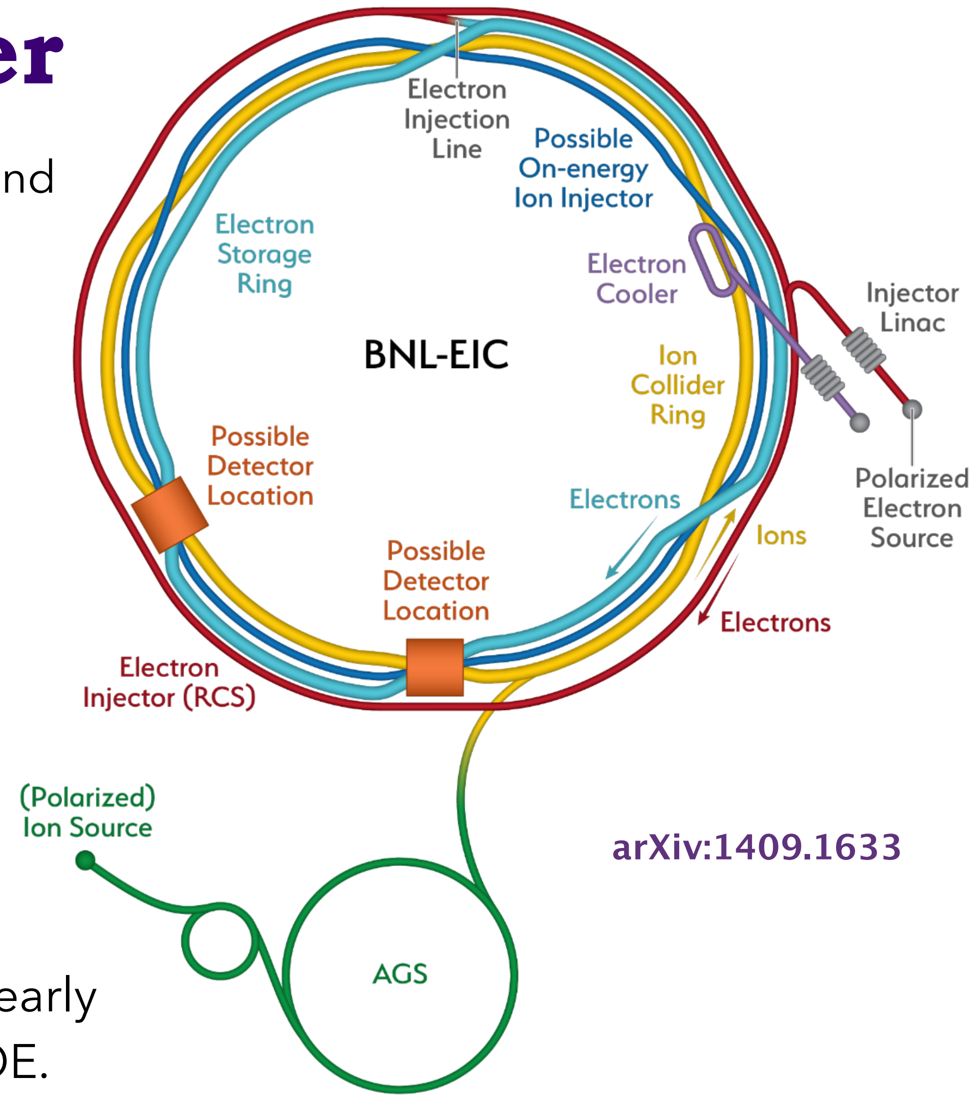

arXiv:1409.1633

Brookhaven National Lab selected as the site early in 2020, following the granting of CD-0 by DOE.

Dedicated studies of EIC physics and design: EIC White Paper, Eur. Phy. J. A 52, 9 (2016)
EIC Yellow Report, https://arxiv.org/abs/2103.05419

EIC kinematic reach: DVCS

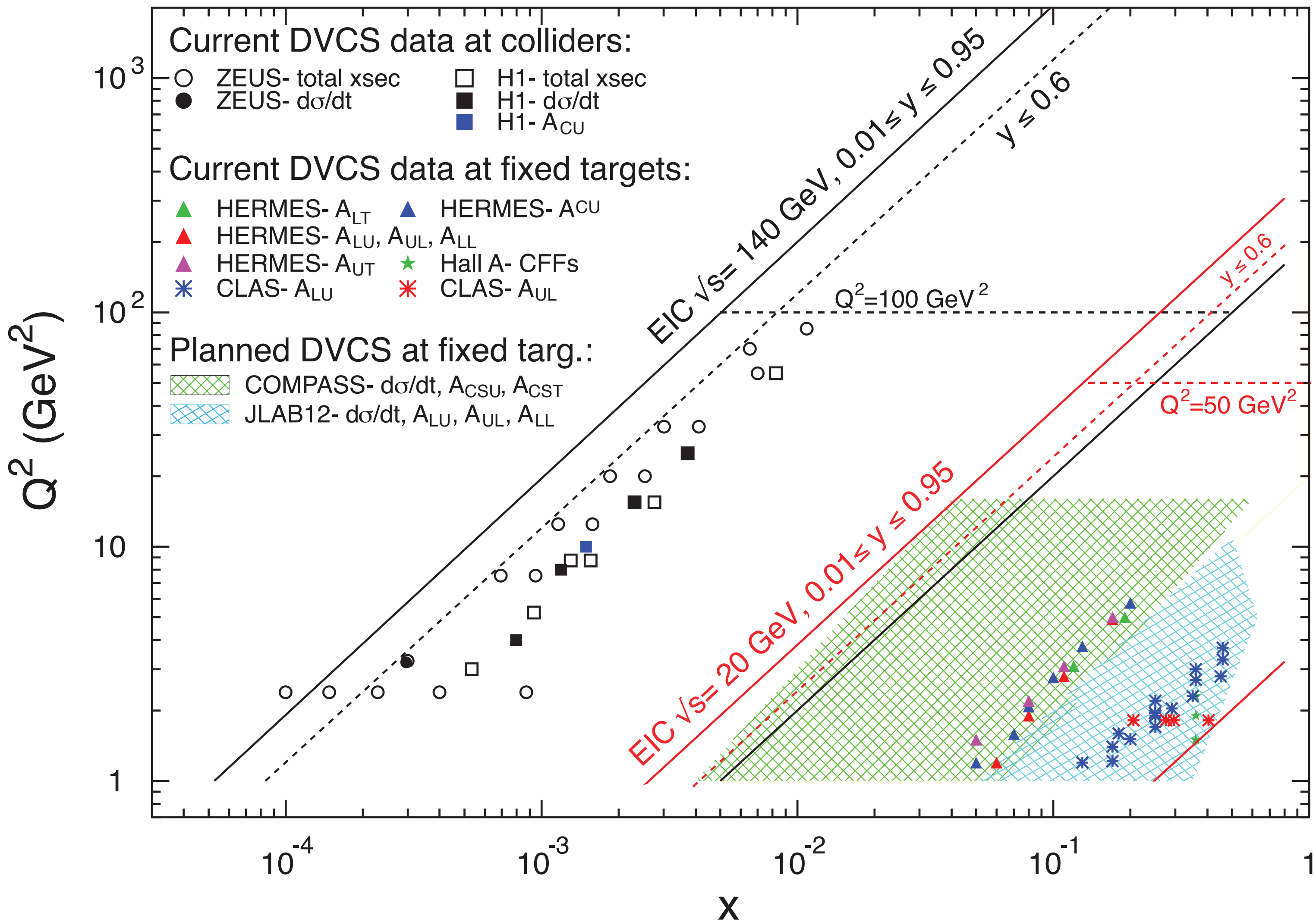

https://arxiv.org/abs/2103.05419

Detector configuration

- Very asymmetric beams

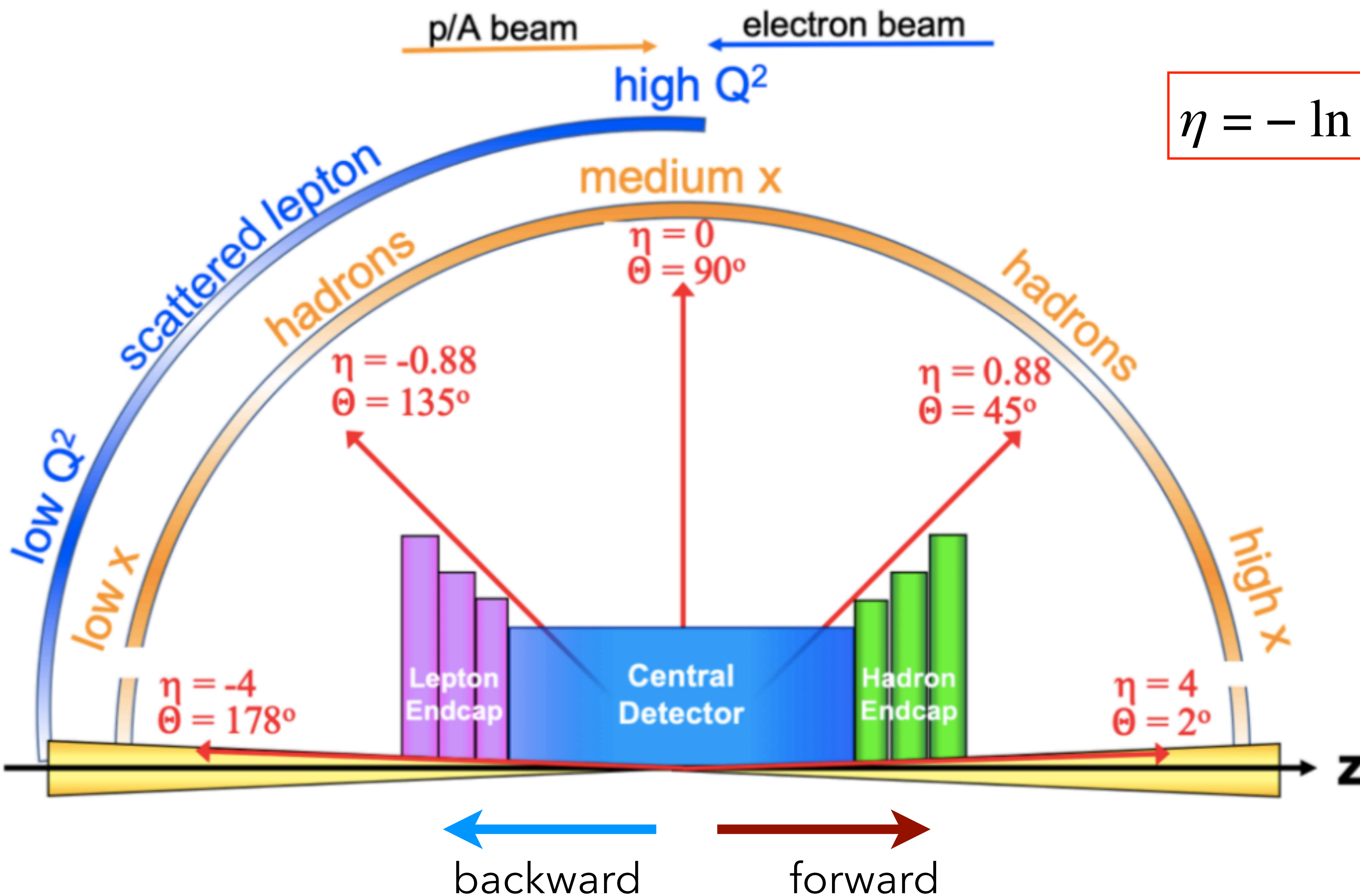

$$\eta = -\ln\tan(\theta/2)$$

Detector requirements

4π hermetic detector with low mass inner tracking.

Central detector, including a solenoid magnet: acceptance in $-4 < \eta < 4$, with full coverage in $|\eta| < 3.5$.

- Tracking and momentum measurement
- Electron ID
- Hadron ID
- Jet energy measurement

Barrel detector ($|\eta| < 1$) + two disc end-caps (forward/hadron end-cap and backward/electron endcap).

Far-backward detectors:

Low-Q^2 tagger (tracker + calorimeter)

Far-forward detectors:

Far from interaction point, very low angles.

Roman Pots inside the beam pipe, B0 tracker for larger anges, large acceptance Zero degree Calorimeter (ZDC) to detect neutrons (nuclear breakup / neutral decay products)

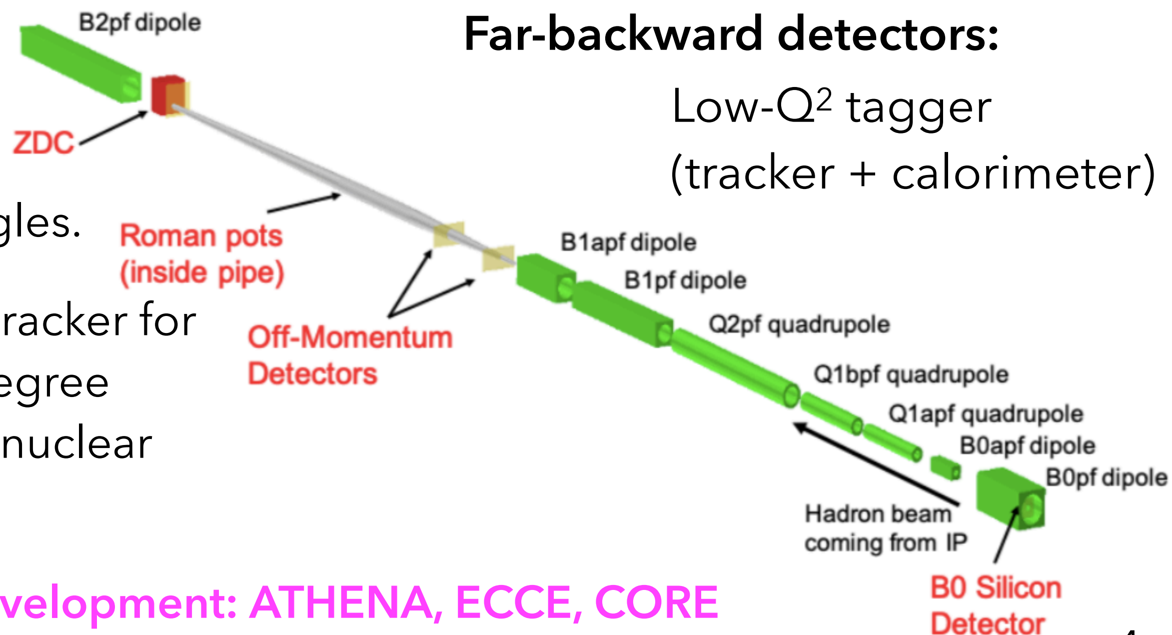

Detector proposals currently under development: ATHENA, ECCE, CORE

Timelike Compton Scattering

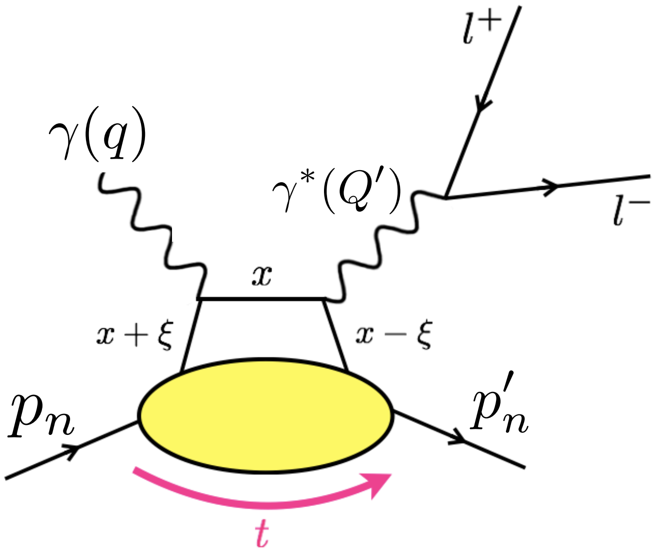

- Time-reversal process of DVCS: parametrised in terms of same Compton Form Factors (their complex conjugates).
  - Verification of GPD universality.
  - Another route to access the D-term.

- Factorisation ensured by hard scale of γ^* virtuality:

$$\frac{t}{Q'^2} << 1$$

$$Q' = l^+ + l^- \qquad \xi = \frac{\tau}{2-\tau}$$

$$s = (q + p_n)^2$$

$$\tau = \frac{Q'^2}{s - m_p^2}$$

θ: angle between l^+ and scattered proton in lepton CMS

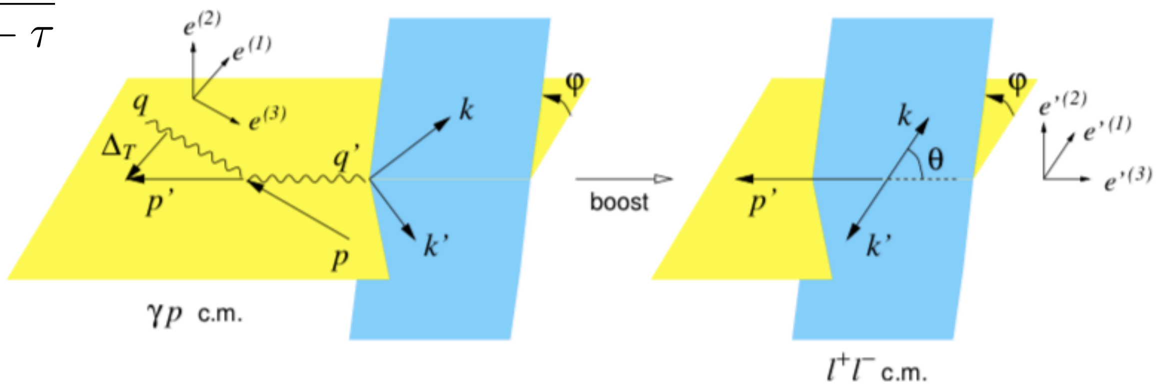

Bethe-Heitler in TCS

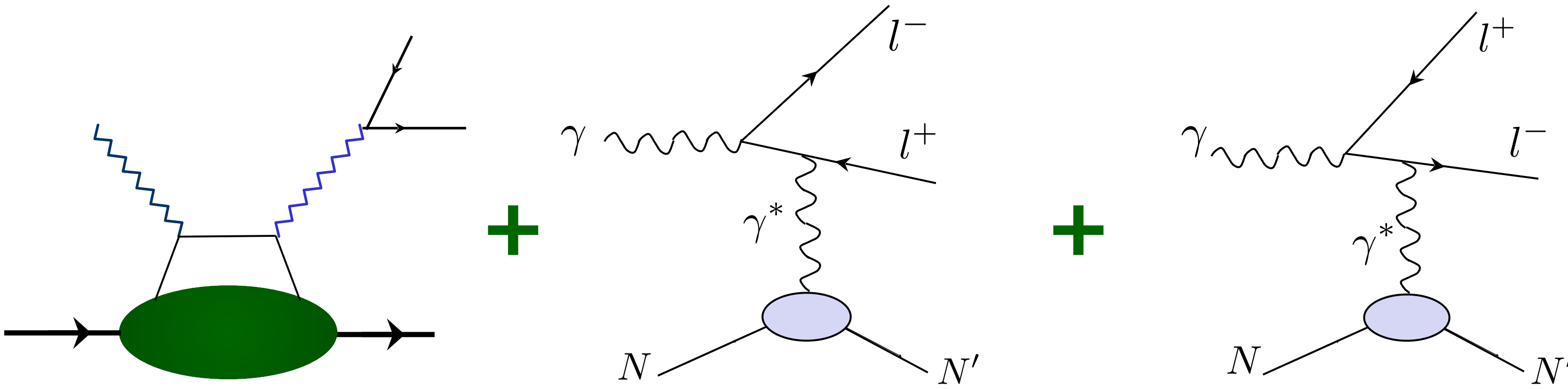

- Similarly to DVCS, TCS process interferes with Bethe-Heitler at the amplitude level.

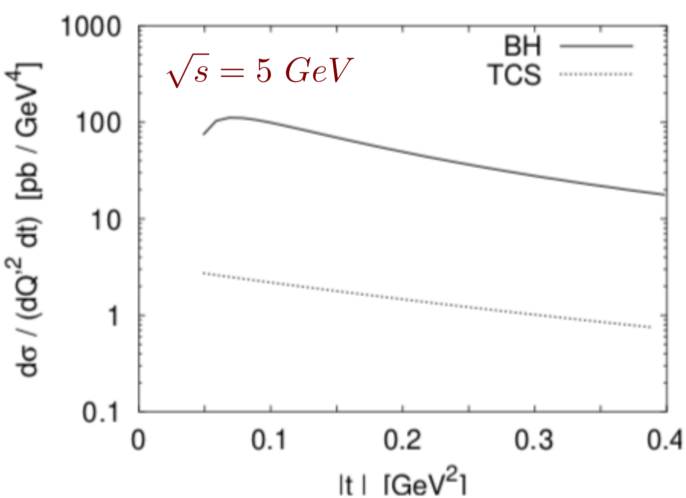

$$\sigma(\gamma p \to p' e^+ e^-) = \sigma_{BH} + \sigma_{TCS} + \sigma_{INT}$$

- Cross-sections hard to obtain! Suppressed by factor of 100 wrt BH.

- Look to other observables.

E.R. Berger, M. Diehl, B. Pire. EPJ C, 23(4):675689 (2002).

TCS observables

- Unpolarised cross-sections:

  sensitive to $\mathcal{Re}\ \mathcal{H}$.

$$\frac{d^4\sigma_{INT}}{dQ'^2 dt d\Omega} = A\frac{1+\cos^2\theta}{\sin\theta}[\cos\phi\ \mathrm{Re}\tilde{M}^{--} - \nu\cdot\sin\phi\ \mathrm{Im}\tilde{M}^{--}]$$

$$\tilde{M}^{--} = \left[F_1\mathcal{H} - \xi(F_1+F_2)\tilde{\mathcal{H}} - \frac{t}{4m_p^2}F_2\mathcal{E}\right]$$

suppressed

- Circularly-polarised photon cross-section: access to $\mathcal{Im}\ \mathcal{H}$.
- More promising observables: asymmetries and cross-section ratios.
- Photon-polarisation (beam-spin) asymmetry:

$$A_{\odot U} = \frac{d\sigma^+ - d\sigma^-}{d\sigma^+ + d\sigma^-}$$

access to $\mathcal{Im}\ \mathcal{H}$

- Forward - backward asymmetry:

$$A_{FB}(\theta,\phi) = \frac{d\sigma(\theta,\phi) - d\sigma(180^\circ-\theta, 180^\circ+\phi)}{d\sigma(\theta,\phi) + d\sigma(180^\circ-\theta, 180^\circ+\phi)}$$

access to $\mathcal{Re}\ \mathcal{H}$

P. Chatagnon et al. (CLAS): arXiv:2108.11746 [hep-ex], *accepted (PRL)*

TCS observables

- The *R* ratio of integrated cross-sections:

Integrated cross-section over θ and φ

$$R(\sqrt{s}, Q'^2, t) = \frac{\int_0^{2\pi} d\phi \cos(\phi) \frac{dS}{dQ'^2 dt d\phi}}{\int_0^{2\pi} d\phi \frac{dS}{dQ'^2 dt d\phi}}$$

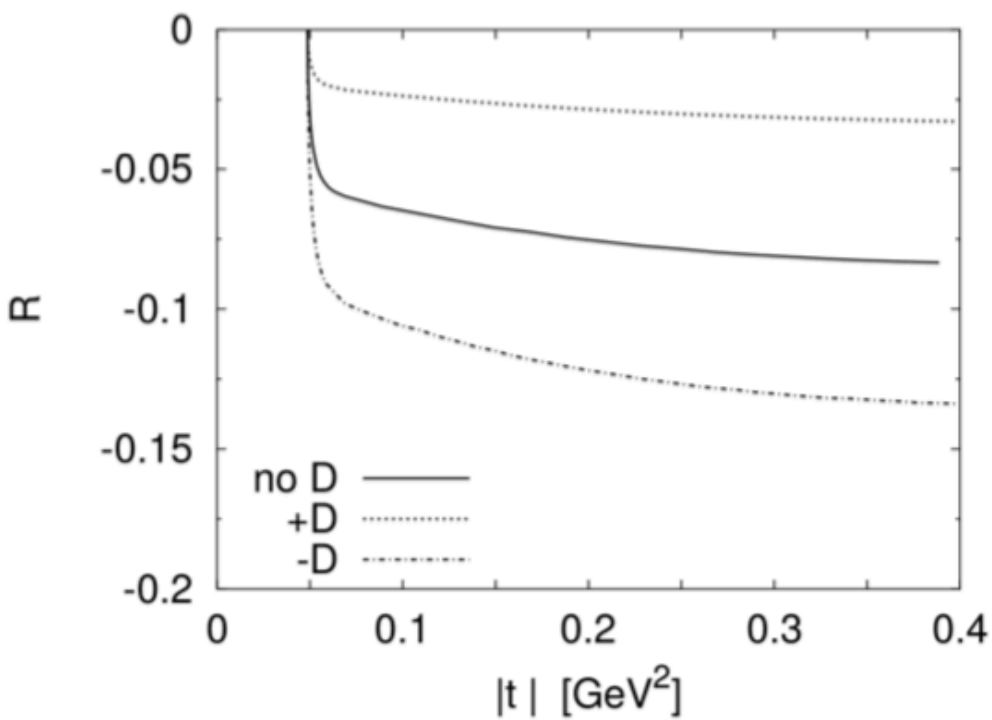

Sensitivity to $\mathcal{R}e\,\mathcal{H}$ and the D-term, but integrated over some of the phase-space: susceptible to detector acceptance effects.

E.R. Berger, M. Diehl, B. Pire. EPJ C, 23(4):675689 (2002).

EpIC: generator

- Generator: EpIC, interfaced to PARTONS, uses CFFs from the GK model.
- Simulations carried out with the ATHENA detector (Geant4).
- Bethe-Heitler dominates by ~factor of 100: generate BH + TCS + Interference

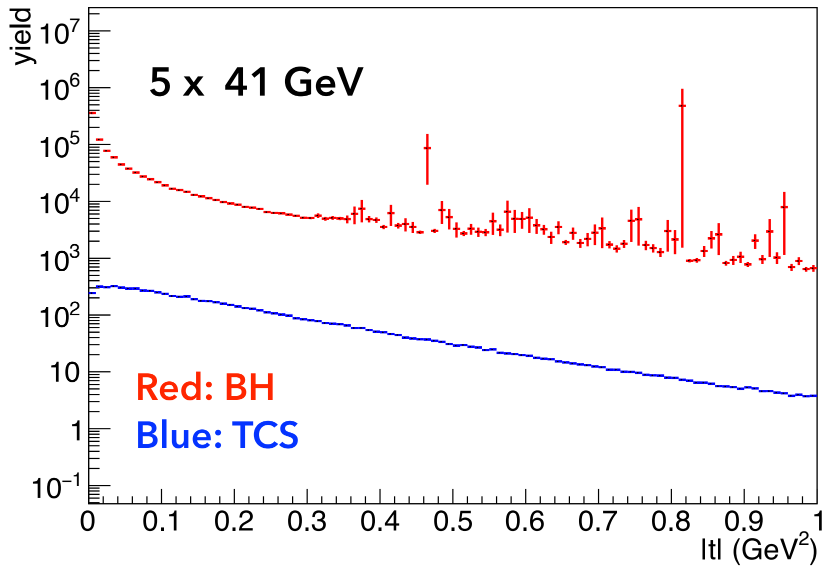

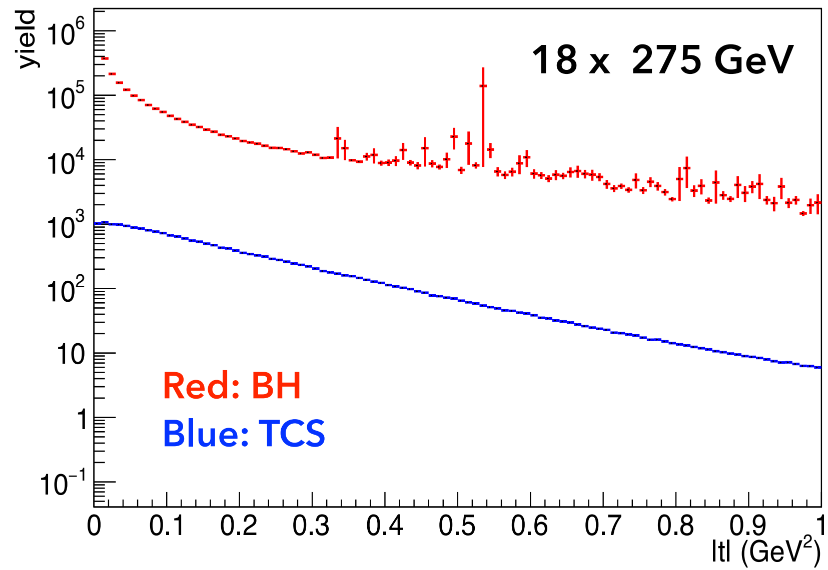

- Generated limits:

$$0 < Q^2 < 0.15\ GeV^2 \qquad 2 < Q'^2 < 20\ GeV^2 \qquad \frac{\pi}{6} < \theta < \frac{5\pi}{6} \qquad \phi : 0 \to 2\pi$$

$$-1 < t < 0\ GeV^2 \qquad 0.01 < y < 0.95 \qquad \phi_s : 0 \to 2\pi$$

Scattered electron

- Scattered electron at very large backward angles: at 5 x 41 GeV only ~ 8% detected in the lepton endcap of the central barrel, at 18 x 275 GeV: none.

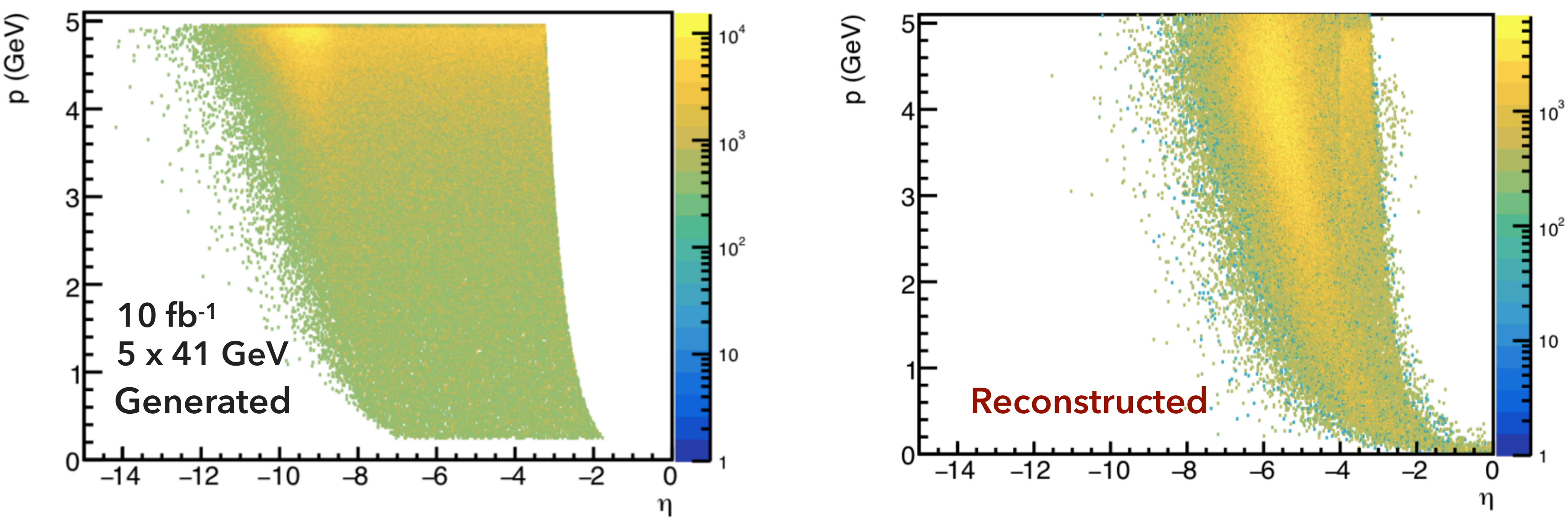

- In most cases, reconstruct through missing mass.

Scattered electron

- Scattered electron at very large backward angles: at 5 x 41 GeV only ~ 8% detected in the lepton endcap of the central barrel, at 18 x 275 GeV: none.

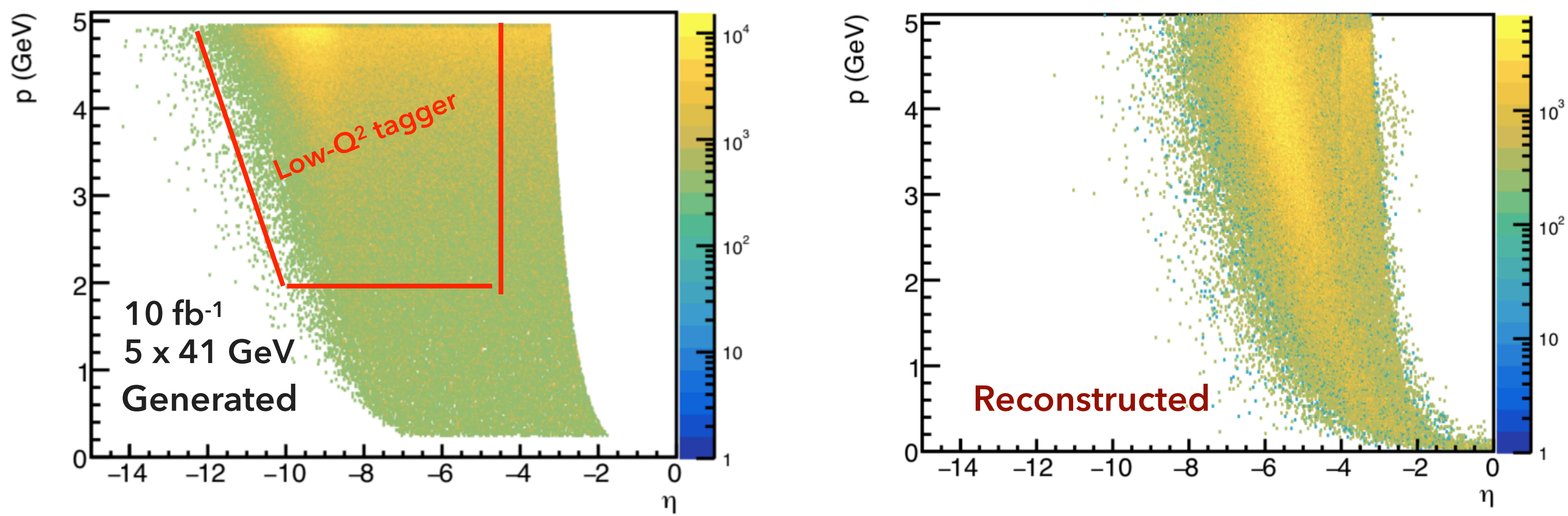

- In most cases, reconstruct through missing mass.

- Possibility of a fully exclusive reconstruction with the addition of a low-Q^2 tagger for the very far-backward angles.

Scattered proton

- Proton recoils at very low forward angle: detected in the Roman Pots and the B0 tracker.

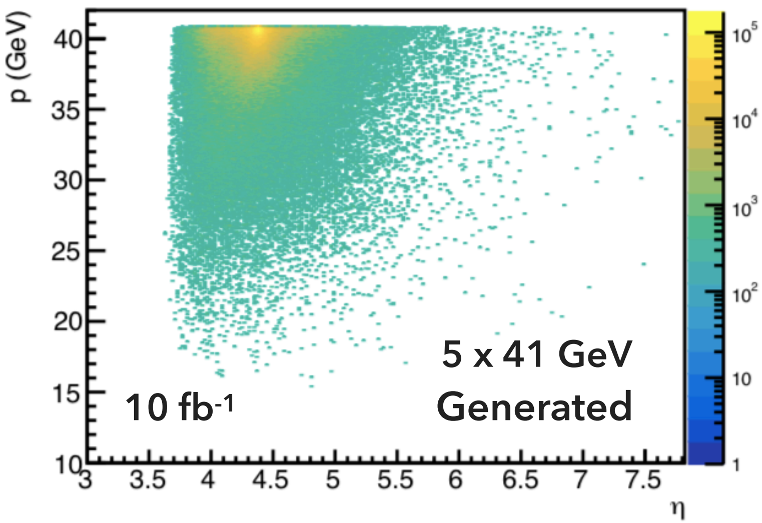

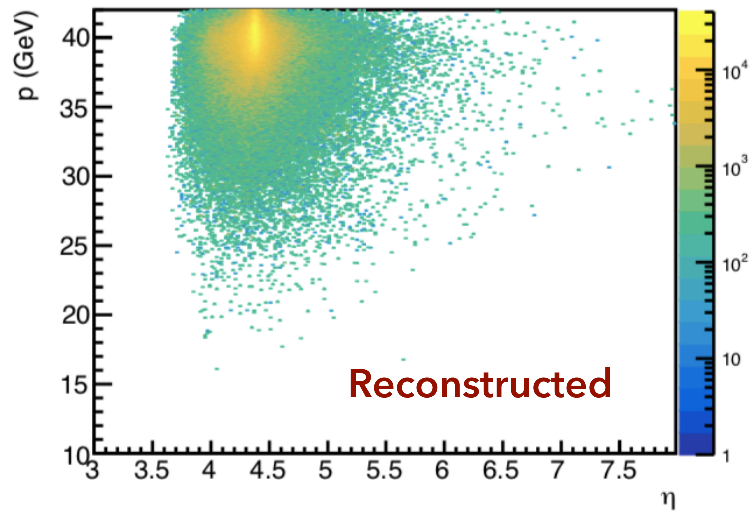

Lab co-ordinates: z-axis defined by the electron beam, proton beam tilted at 25mrad to it (crossing angle).

Excellent efficiency and acceptance

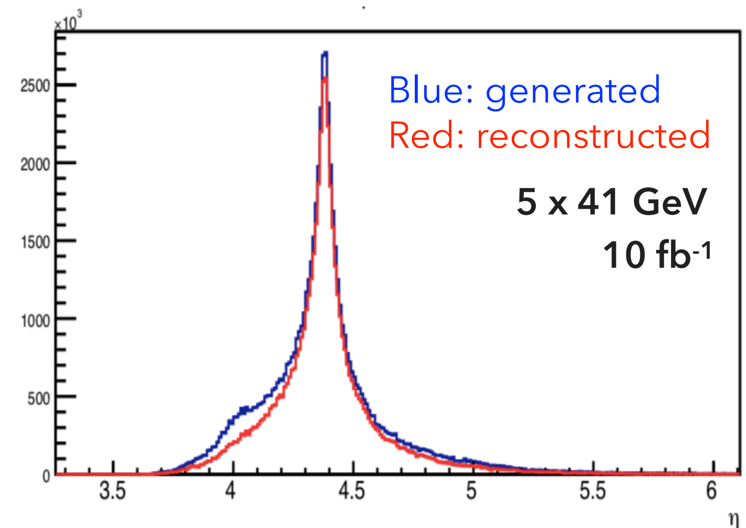

Produced leptons: e^+e^-

- Detected by the trackers and calorimeters in the central barrel.
- Efficiency for 5x41 GeV collisions: ~ 91%

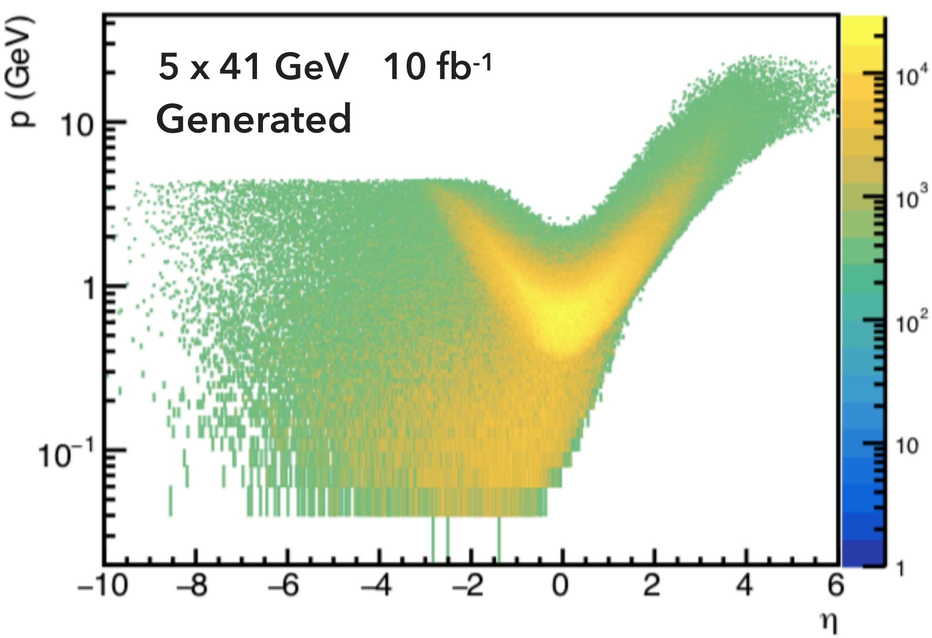

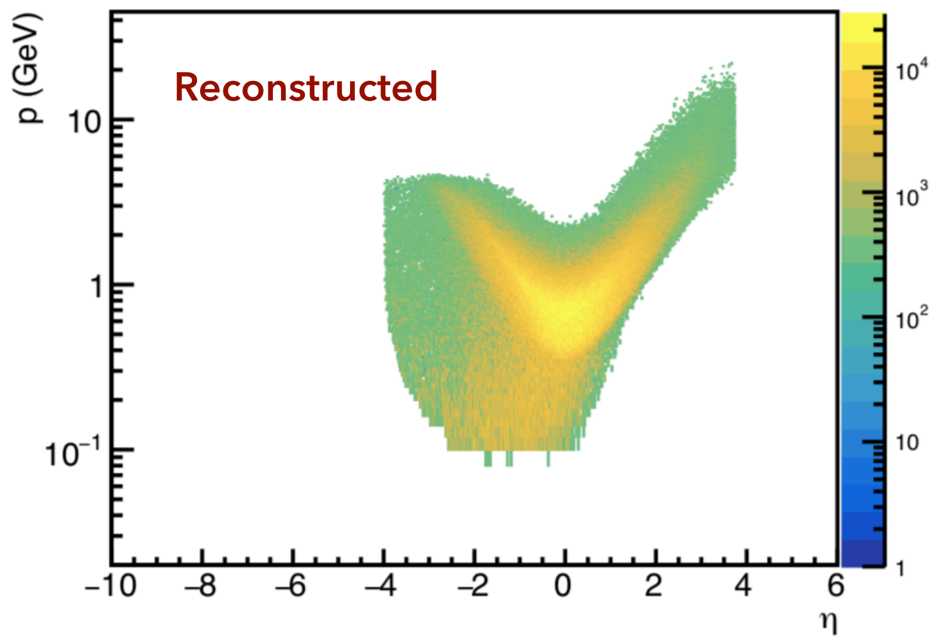

Kinematics

- 5 x 41 GeV, 10 fb^{-1}

blue: generated, red: reconstructed

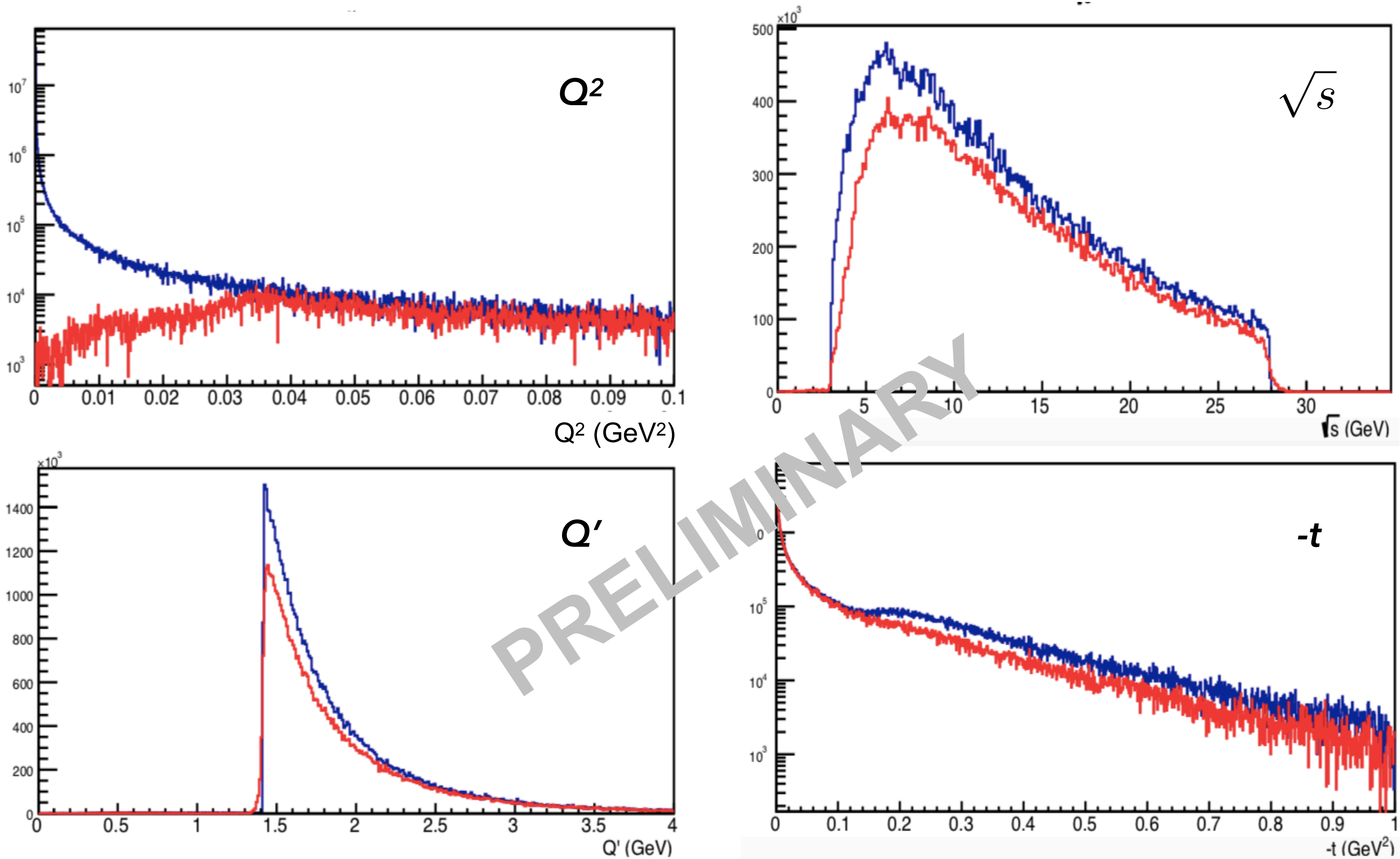

Kinematics

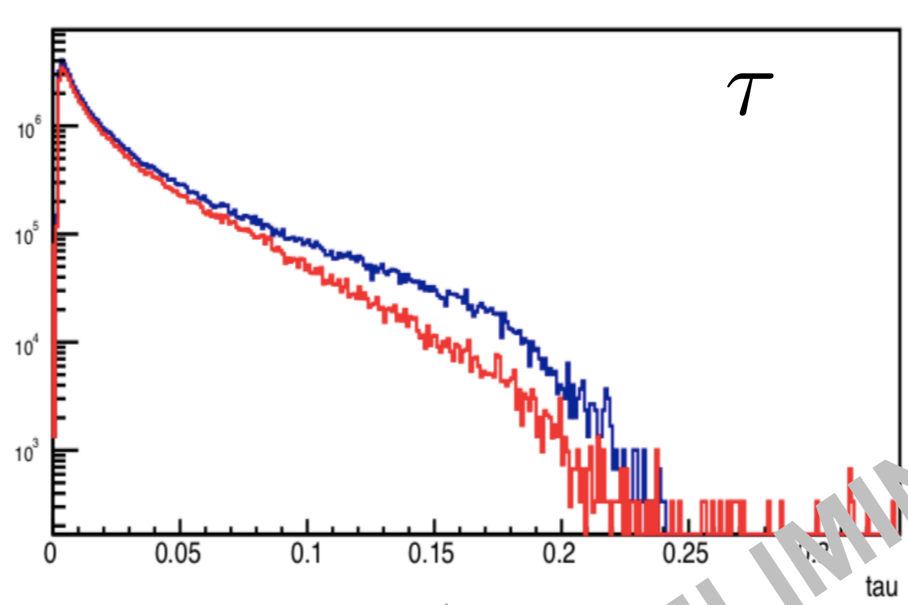

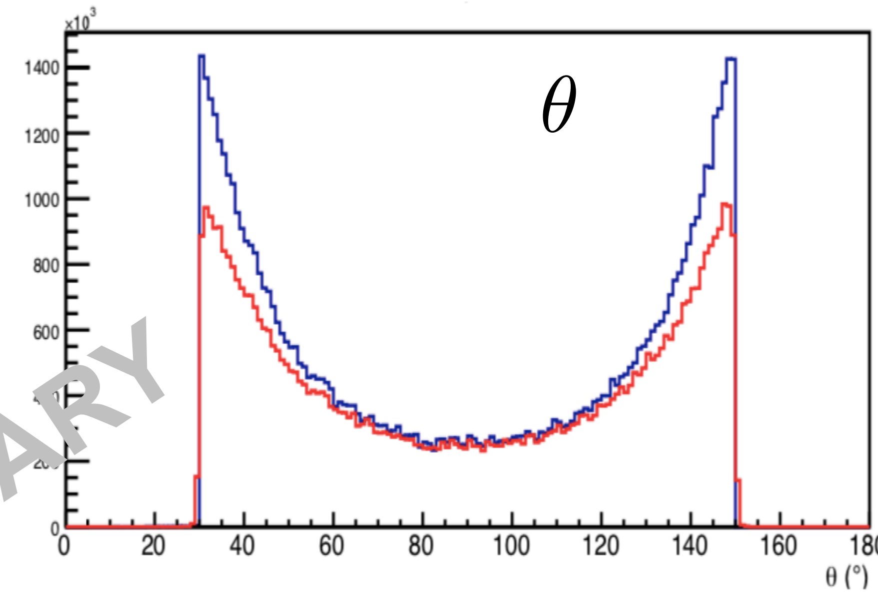

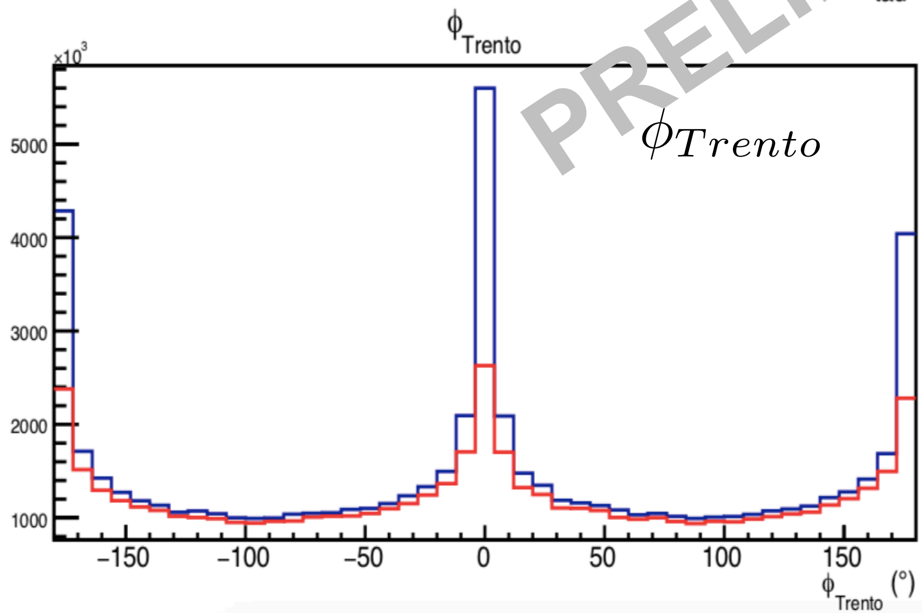

5 x 41 GeV, 10 fb^{-1}

blue: generated

red: reconstructed

Integrated efficiency: 84%.

Beam-spin asymmetry

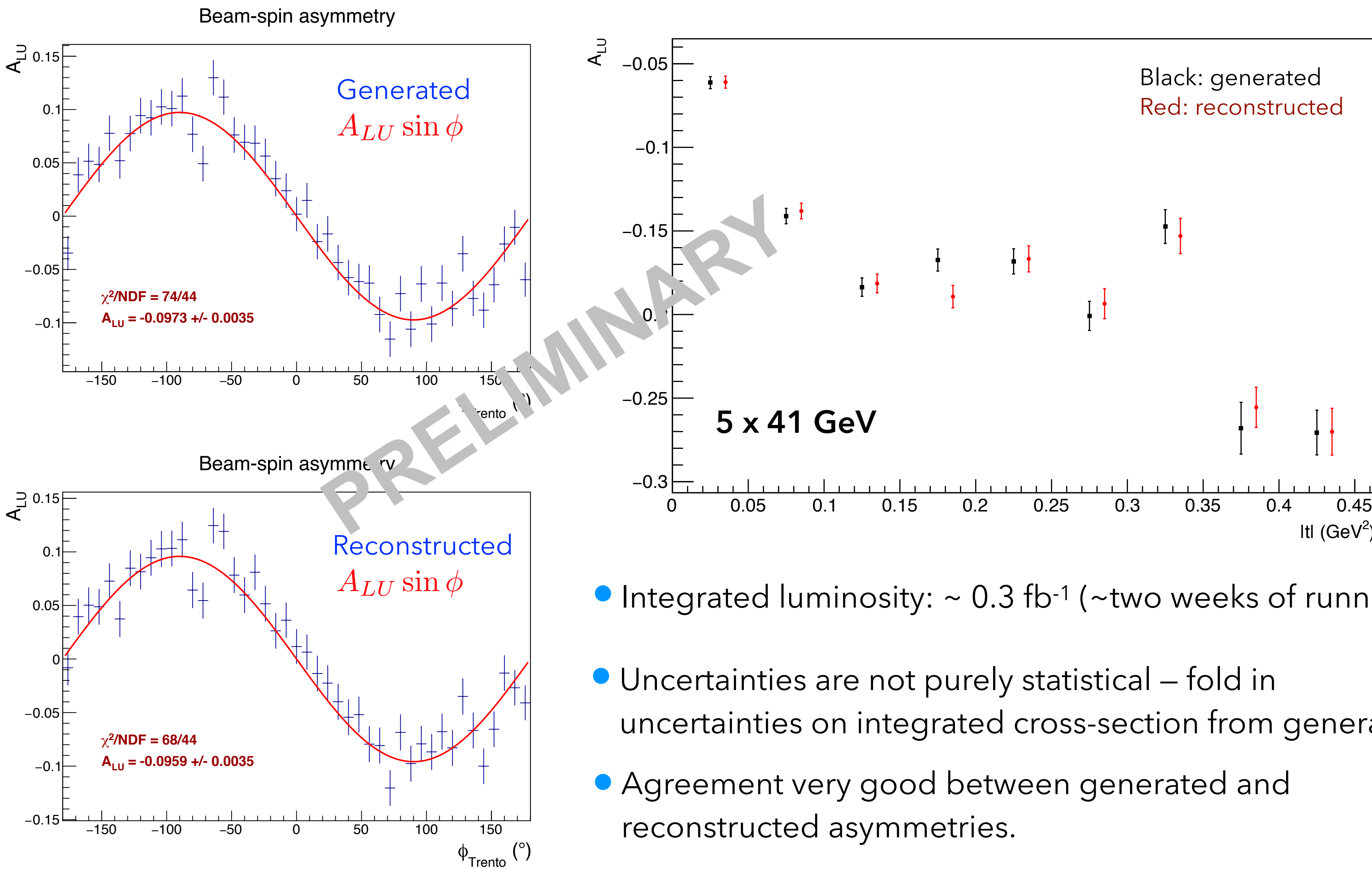

- Integrated luminosity: ~ 0.3 fb^{-1} (~two weeks of running).
- Uncertainties are not purely statistical – fold in uncertainties on integrated cross-section from generator.
- Agreement very good between generated and reconstructed asymmetries.

J/Psi electro-production

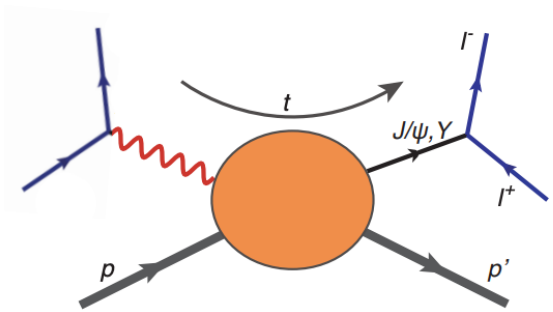

Sensitive to gluon GPDs

Fully exclusive reconstruction: scattered electron detected in the central barrel.

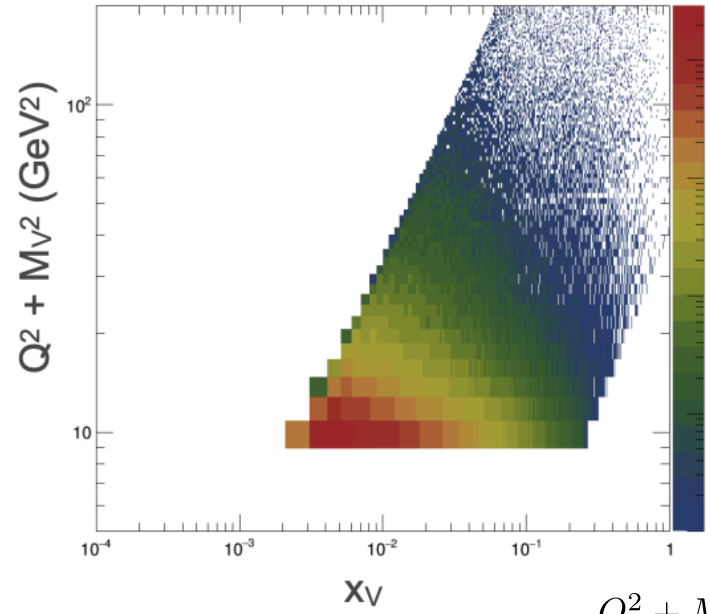

10 x 100 GeV, 10 fb^{-1}

$$x_v = \frac{Q^2 + M_v^2}{2P \cdot q}$$

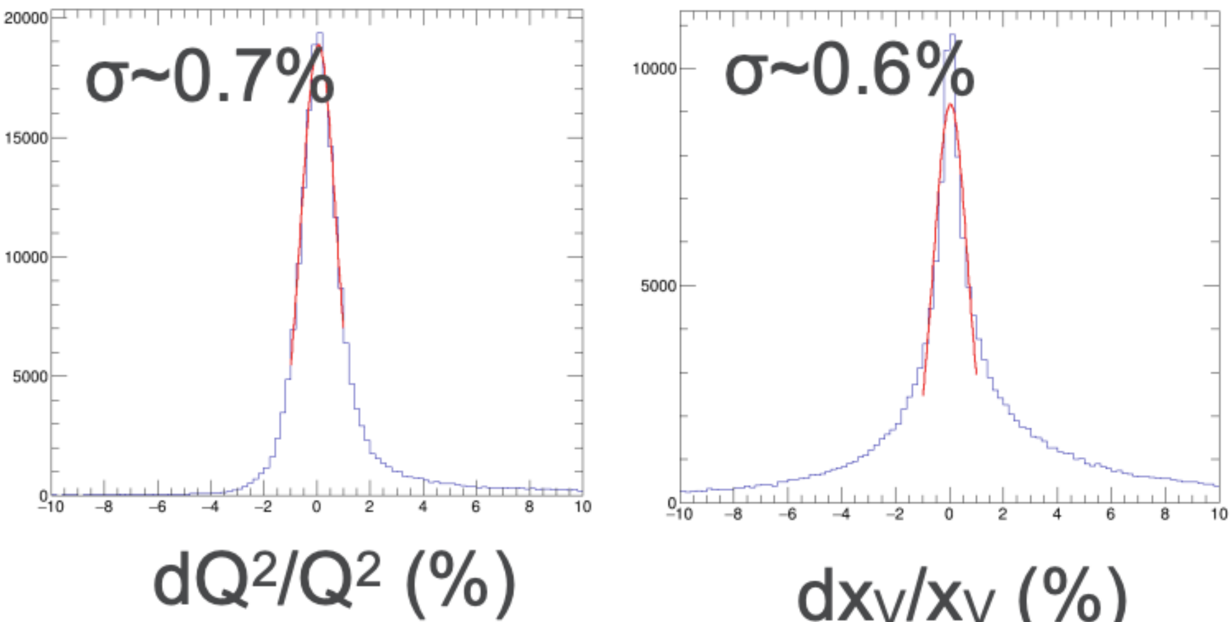

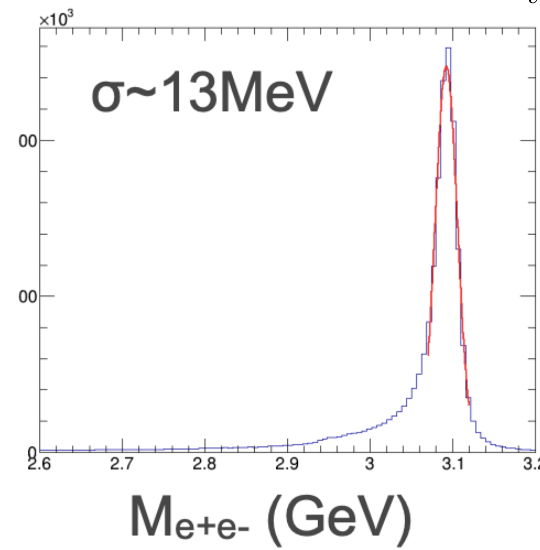

Sylvester Joosten, Chao Peng, Shivangi Prasad (ANL)

J/Psi electro-production

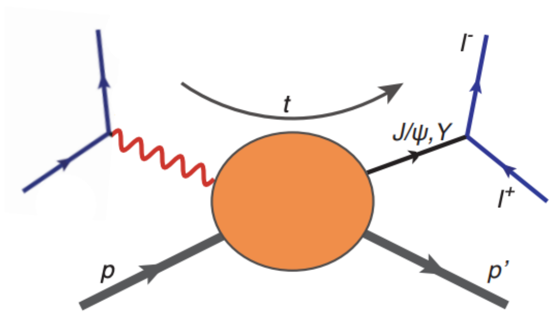

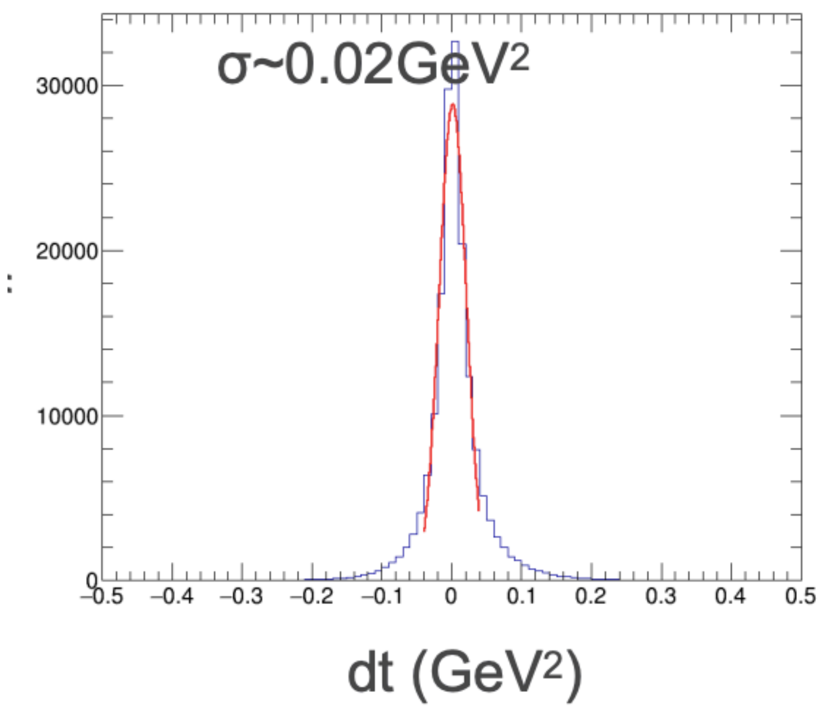

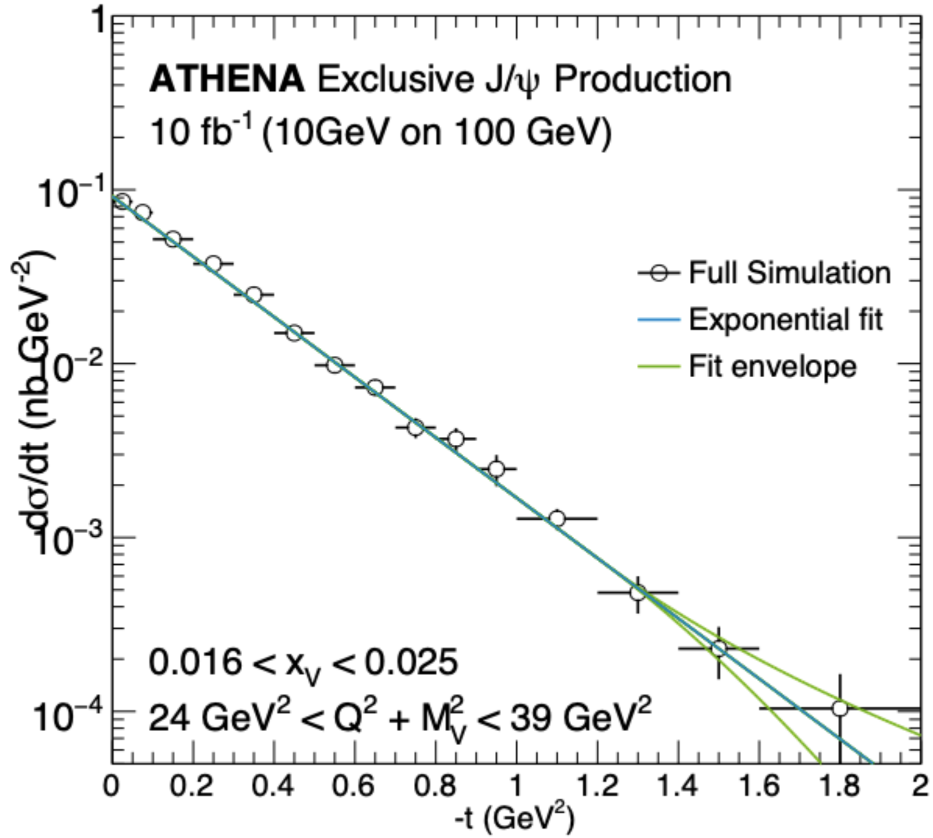

10 x 100 GeV, 10 fb^{-1}

Sylvester Joosten, Chao Peng, Shivangi Prasad (ANL)

Concluding remarks

- Detector proposals are currently being developed for the EIC – decision on the first detector will be taken early in 2022.
- Full detector simulations exist for ATHENA and ECCE.
- At EIC kinematics, Bethe-Heitler dominates over TCS by two orders of magnitude: focus on observables sensitive to BH-TCS interference (asymmetries).
- Measurement of BH-TCS interference possible at ATHENA (*also ECCE, not shown*) with good acceptance and efficiency. Backgrounds not yet studied.
- Scattered electron at very low angles: reconstruct via missing mass or low-Q^2 tagger.
- J/Psi electro-production possible: fully exclusive, wide scan in t.
- Possibility to detect muons in ATHENA: could almost double the stats via the pair-production of muons in TCS or J/Psi.


Thank you!

A constructivist view of the nucleon

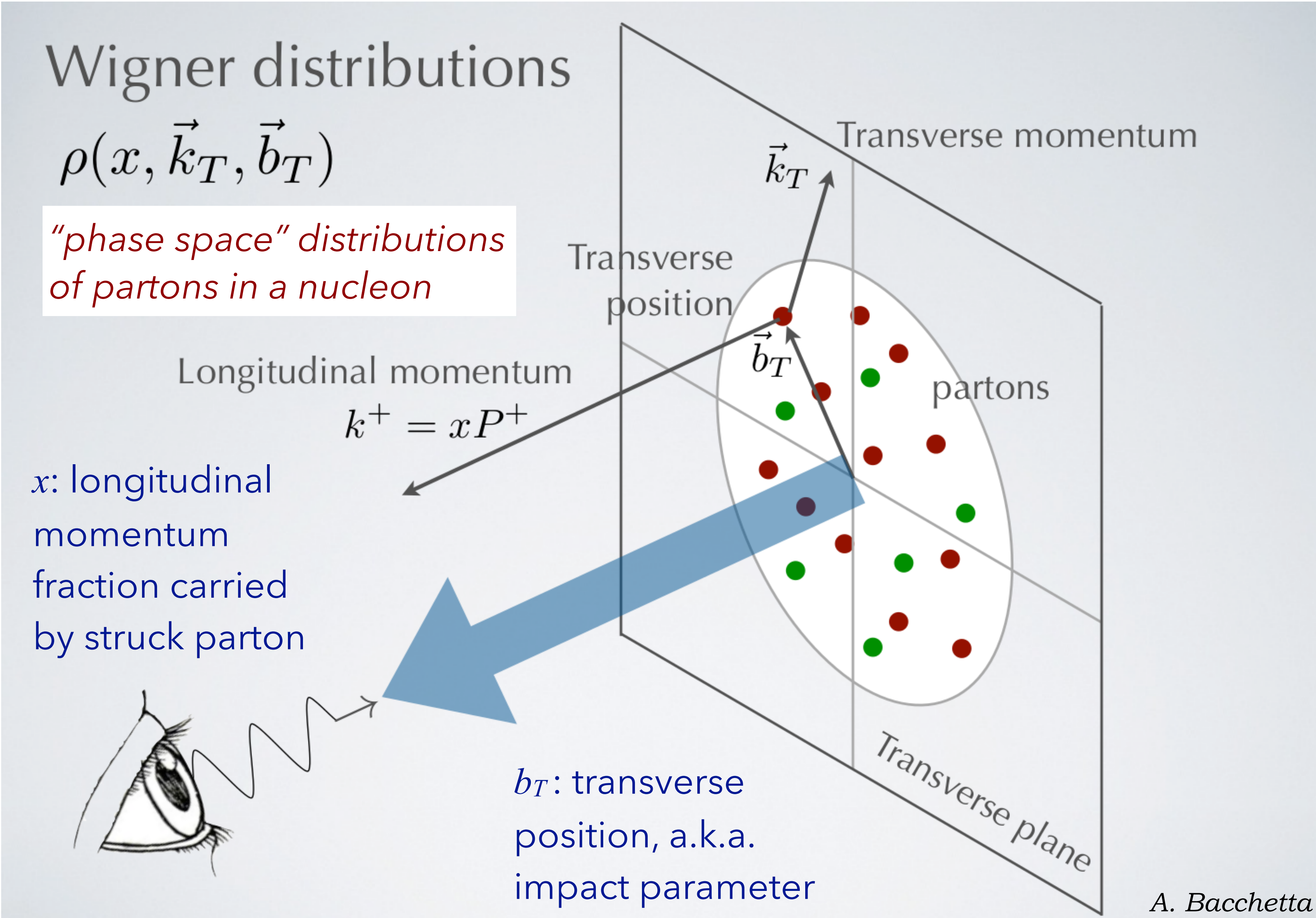

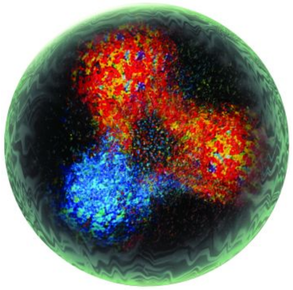

Wigner function: full phase space parton distribution of the nucleon

Generalised Transverse Momentum Distributions (GTMDs)

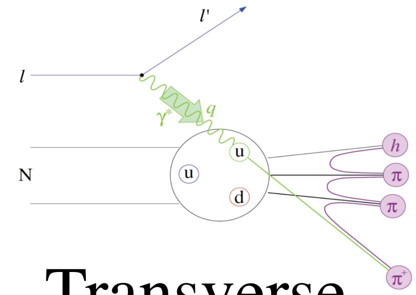

$\int d^2 k_T$

$\int d^2 b_T$

Generalised Parton Distributions (GPDs)

Transverse Momentum Distributions (TMDs)

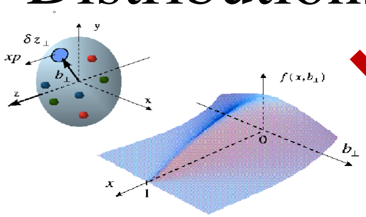

$\int dx$

$\int d^2 b_T$

$\int d^2 k_T$

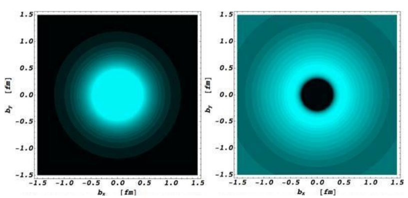

Form Factors

eg: G_{E}, G_{M}

Parton Distribution Functions (PDFs)

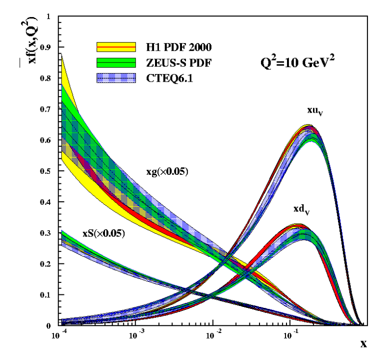

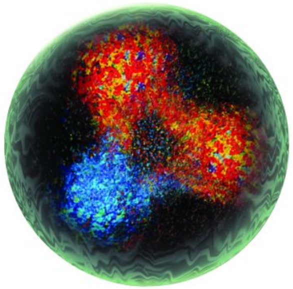

Wigner function: full phase space parton distribution of the nucleon

Generalised Transverse Momentum Distributions (GTMDs)

$\int d^2 k_T$

$\int d^2 b_T$

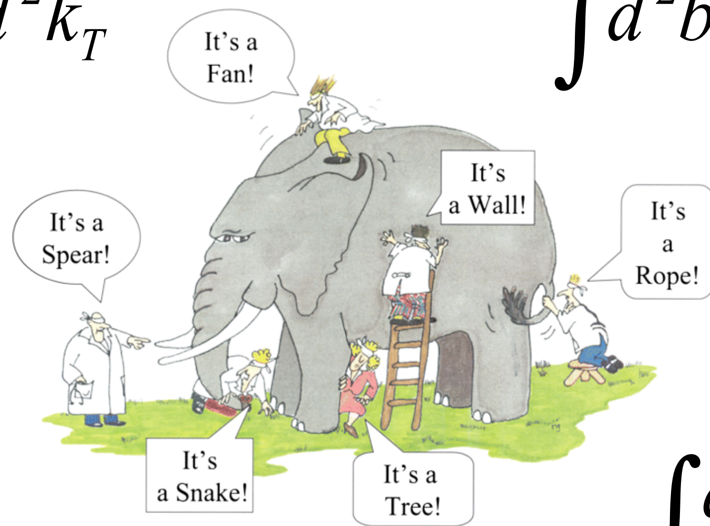

G. Renee Guzlas, artist.

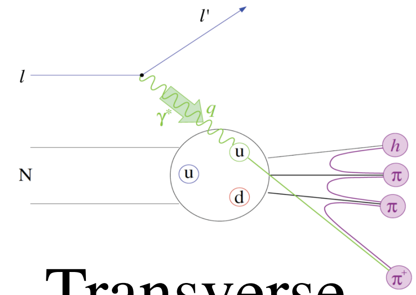

Transverse Momentum Distributions (TMDs)

Generalised Parton Distributions (GPDs)

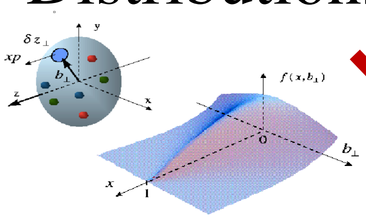

$\int dx$

$\int d^2 k_T$

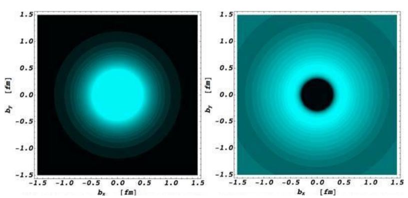

Form Factors

eg: G_E, G_M

Parton Distribution Functions (PDFs)

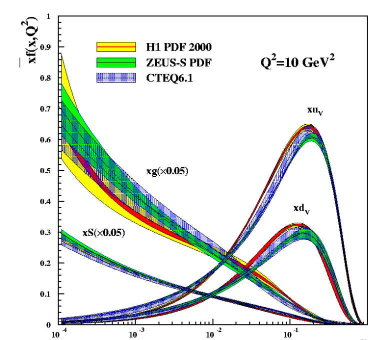

Generalised Parton Distributions (GPDs) —
proposed by Müller (1994), Radyushkin, Ji (1997).

✱ *Directly related to the matrix element of the energy-momentum tensor evaluated between hadron states.*

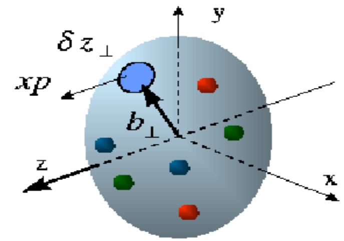

In the infinite momentum frame, can be interpreted as relating transverse position of partons (impact parameter), $b_\perp$, to their longitudinal momentum fraction (x).

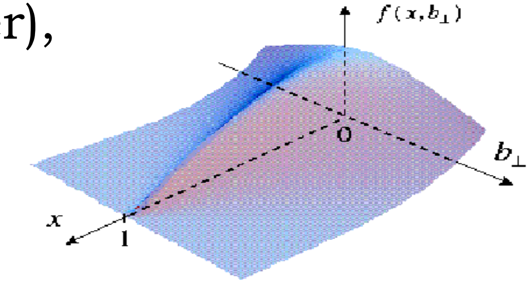

Tomography: 3D image of the nucleon.

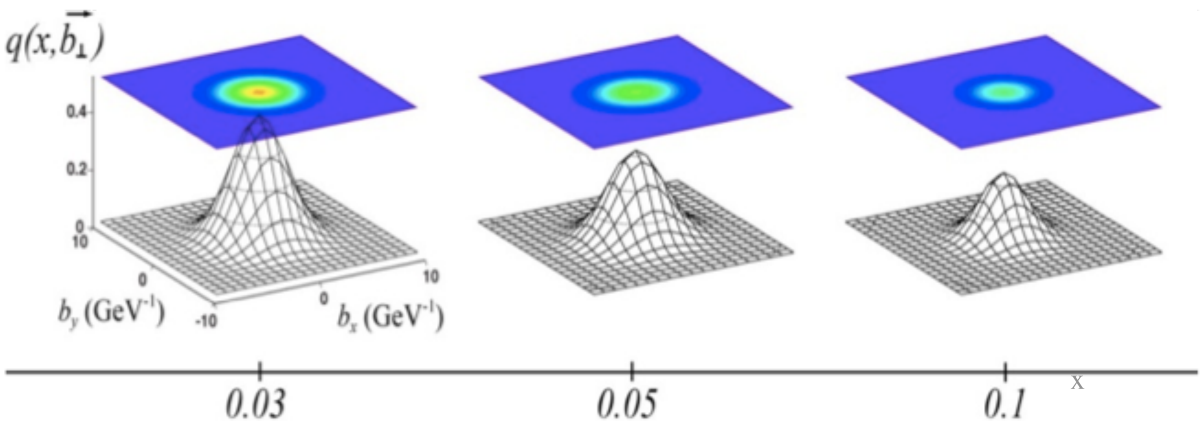

✱ First studies at JLab and DESY (HERMES), currently at JLab and CERN (COMPASS). A crucial part of the JLab12 programme — and, in the future, of the EIC.

Experimental access to GPDs

Accessible in *exclusive* processes, where all final state particles are determined, *eg*:

- Deeply Virtual Compton Scattering (DVCS)
- Time-like Compton Scattering (TCS)
- Hard Exclusive Meson Production (HEMP) – a.k.a. Deeply Virtual Meson Production (DVMP)
- Double DVCS
- Certain diffractive processes, eg: diffractive ρ-production with the emission of a meson or virtual photon from the nucleon
- Hard exclusive production of a meson-photon or photon-photon pair
- Charged-current meson production, eg: $ep \to \nu_e \pi^- p$

Relies on *factorisation* of the process amplitude into a hard, perturbative part and the soft non-perturbative part containing GPD information.

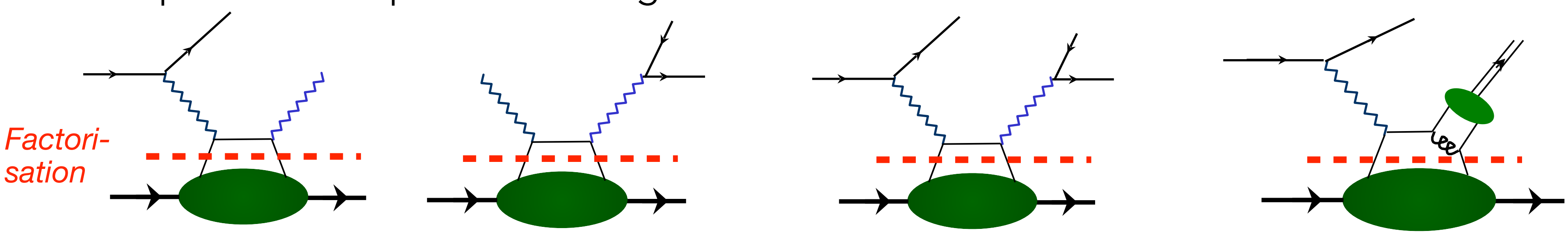

DVCS

Virtual photon space-like

TCS

Virtual photon time-like

DDVCS

One time-like, one space-like virtual photon

DVMP

Virtual photon space-like

Deeply Virtual Compton Scattering

the "golden channel" for GPD extraction

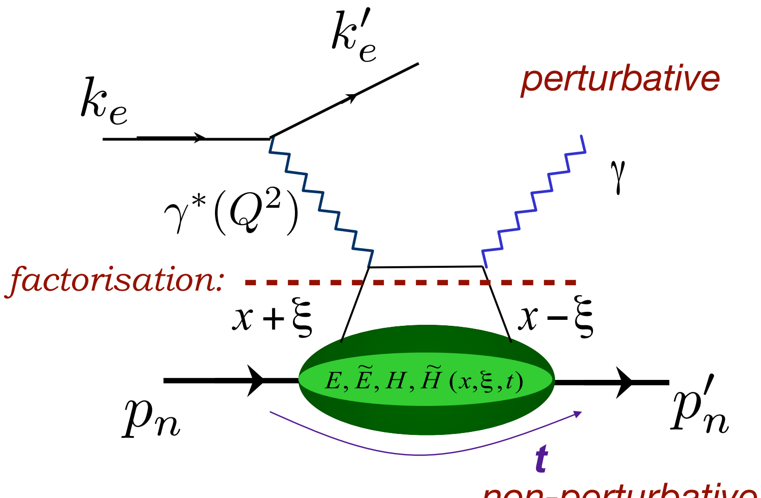

"Handbag" diagram

$$Q^2 = -(\mathbf{k} - \mathbf{k}')^2 \qquad t = (\mathbf{p'_n} - \mathbf{p_n})^2$$

Bjorken variable: $x_B = \dfrac{Q^2}{2\mathbf{p_n}\cdot\mathbf{q}}$

$x \pm \xi$ *longitudinal momentum fractions of the struck parton*

Skewness: $\xi \cong \dfrac{x_B}{2 - x_B}$

* At high exchanged Q^2 and low t access to four parton helicity-conserving, chiral-even GPDs:

$$E^q, \tilde{E}^q, H^q, \tilde{H}^q(x, \xi, t)$$

* Can be related to PDFs:

$$H(x,0,0) = q(x) \quad \tilde{H}(x,0,0) = \Delta q(x)$$

and form factors:

$$\int_{-1}^{+1} H dx = F_1 \qquad \int_{-1}^{+1} \tilde{H}\, dx = G_A$$

$$\int_{-1}^{+1} E\, dx = F_2 \qquad \int_{-1}^{+1} \tilde{E}\, dx = G_P$$

(Dirac and Pauli) *(axial and pseudo-scalar)*

* Small changes in nucleon transverse momentum allows mapping of transverse structure at large distances.

Measuring DVCS

- Process measured in experiment:

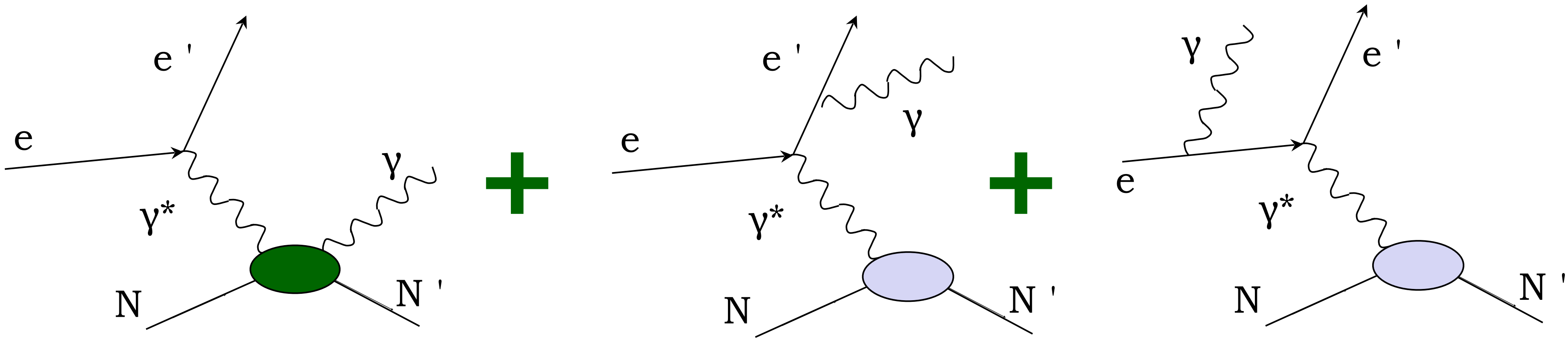

DVCS

Bethe - Heitler

$$d\sigma \propto \left|T_{DVCS}\right|^2 + \left|T_{BH}\right|^2 + T_{BH}T^*_{DVCS} + T_{DVCS}T^*_{BH}$$

Amplitude parameterised in terms of Compton Form Factors

Amplitude calculable from elastic Form Factors and QED

Interference term

$$\left|T_{DVCS}\right|^2 << \left|T_{BH}\right|^2$$

Compton Form Factors in DVCS

Experimentally accessible in DVCS cross-sections and spin or charge asymmetries, eg:

$$A_{LU} = \frac{d\vec{\sigma} - d\overleftarrow{\sigma}}{d\vec{\sigma} + d\overleftarrow{\sigma}} = \frac{\Delta\sigma_{LU}}{d\vec{\sigma} + d\overleftarrow{\sigma}}$$

At leading twist, leading order:

$$T^{DVCS} \sim \int_{-1}^{+1} \frac{GPDs\ (x,\xi,t)}{x \pm \xi + i\varepsilon} dx + \ldots \sim P\int_{-1}^{+1} \frac{GPDs\ (x,\xi,t)}{x \pm \xi} dx \pm i\pi GPDs\ (\pm\xi,\xi,t) + \ldots$$

cross-sections,
beam-charge and
double polarisation asymmetries

single-spin
asymmetries

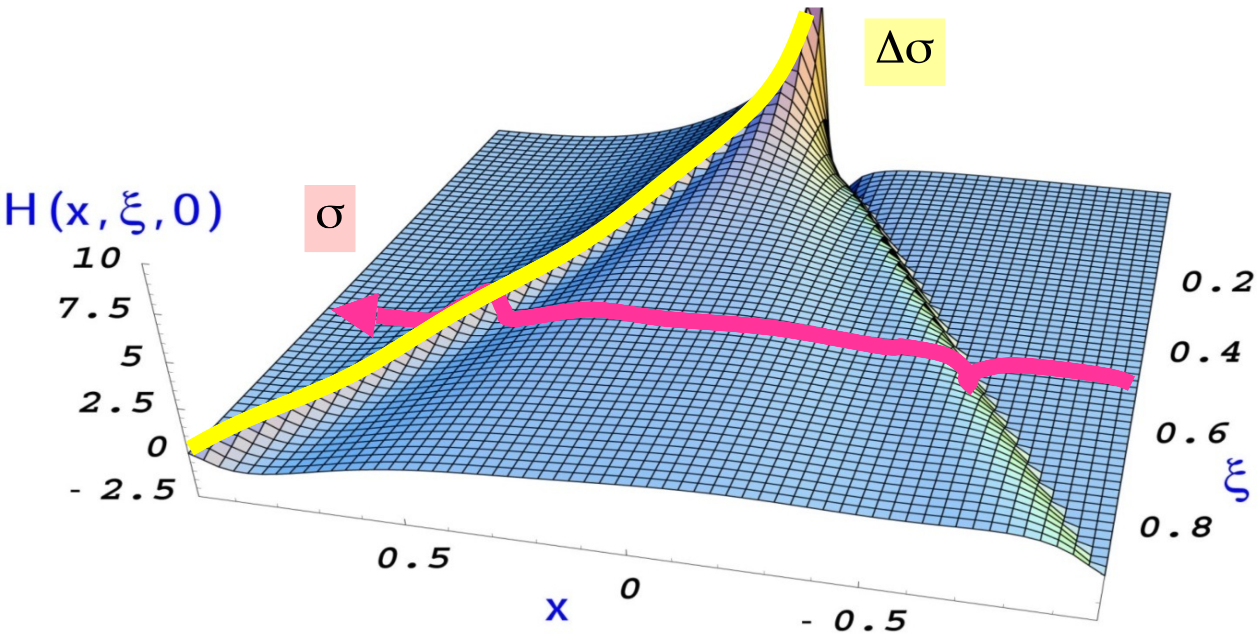

Only ξ and t are accessible experimentally!

To get information on x need extensive measurements in Q^2.

Need measurements off proton and neutron to get flavour separation of CFFs in DVCS.

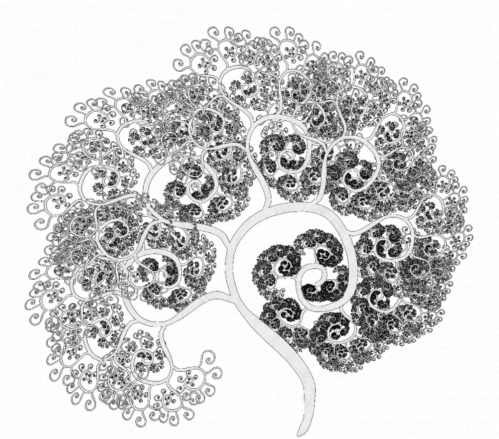

Spontaneousfantasia.com

Order and Twist

Leading order (LO)

Next-to-leading order (NLO)

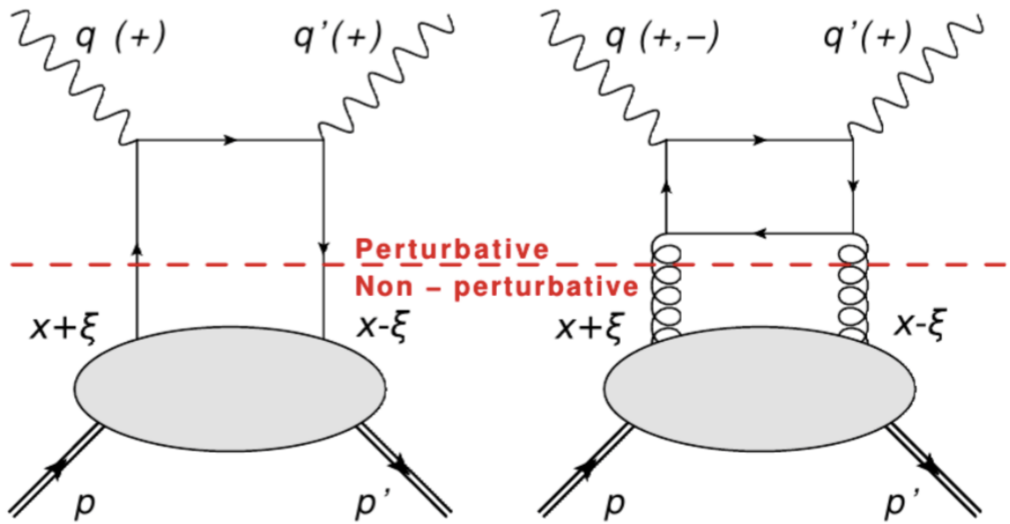

- Twist: powers of $\frac{1}{\sqrt{Q^2}}$ in the DVCS amplitude. Leading-twist (LT) is twist-2.

- Order: introduces powers of α_s

- Leading Order (LO) requires $Q^2 >> M^2$ (M: target mass)

Nucleon Tomography from GPDs

- At a fixed Q^2, x_B, slope of GPD with t is related, via a Fourier Transform, to the transverse spatial spread.

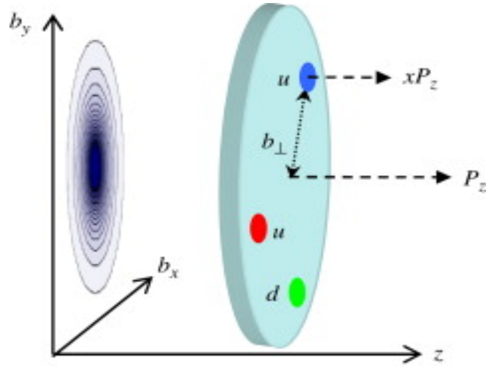

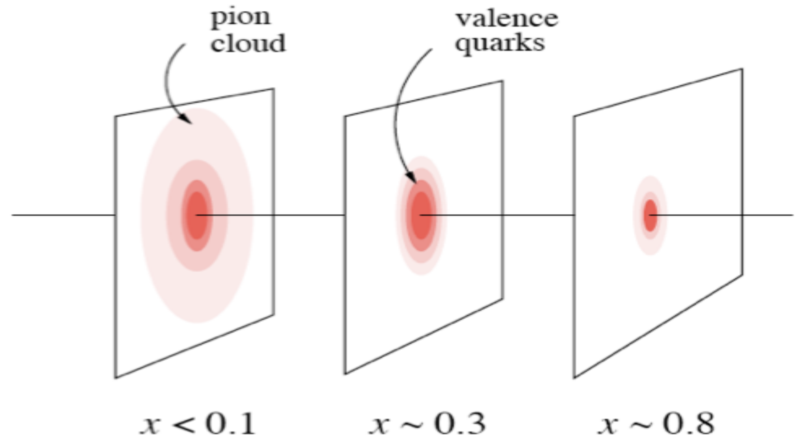

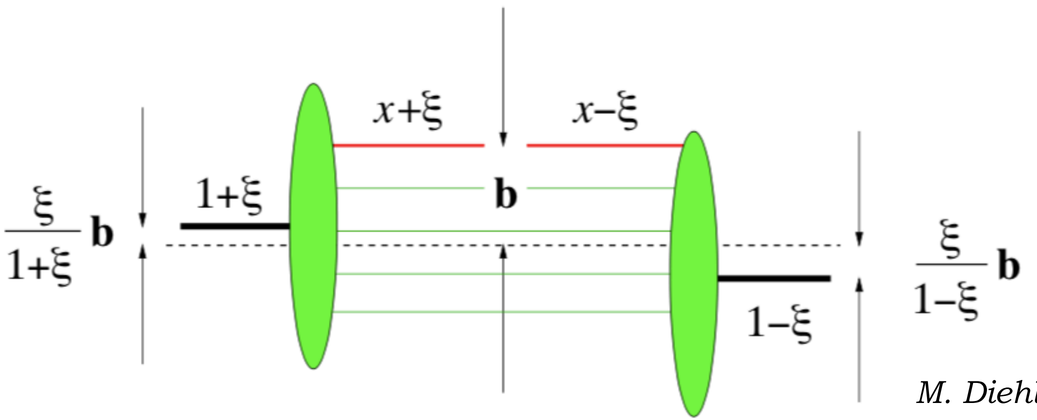

M. Diehl

Formally, the radial separation, **b**, *between the struck parton and the centre of momentum of the remaining spectators.*

- Experimentally, fit the t-dependence of CFFs or structure functions (from HEMP) with an exponential.

eg: $$\frac{d\sigma_U}{dt} = Ae^{Bt}$$

Spin and pressure in the nucleon

- GPDs also provide indirect access to mechanical properties of the nucleon (encoded in the gravitational form factors, GFFs, of the energy-momentum tensor).

  X. D. Ji, PR**D 55**, 7114-7125 (1997)
  M. Polyakov, PL**B 555**, 57-62 (2016)

- Three scalar GFFs, functions of *t*: encode pressure and shear forces ($d_1(t)$), mass ($M_2(t)$) and angular momentum distributions ($J(t)$).

- Can be related to GPDs via sum rules: $$\int x\,[H(x,\xi,t)+E(x,\xi,t)]\,\mathrm{d}x = 2J(t)$$

$$\int xH(x,\xi,t)\mathrm{d}x = M_2(t) + \frac{4}{5}\xi^2 d_1(t)$$

(Ji's relation)

$$J_N = \frac{1}{2} = \frac{1}{2}\Sigma_q + L_q + J_g$$

- $d_1(t)$ (D-term) "last unknown global property of the nucleon" – may can be accessed via the $\mathcal{Re}$ and $\mathcal{Im}$ $\mathcal{H}$:

Dispersion relation: $$\mathrm{Re}\mathcal{H}(\xi,t) = \int_{-1}^{1}\left(\frac{1}{\xi-x}-\frac{1}{\xi+x}\right)\mathrm{Im}\mathcal{H}(\xi,t)\ dx + \Delta(t).$$

Assuming double-distribution parametrisation: $\Delta(t) \propto d_1(t)$

Nucleon at different scales

Valence quarks

Jefferson Lab: fixed-target electron scattering

$0.1 < x_B < 0.7$

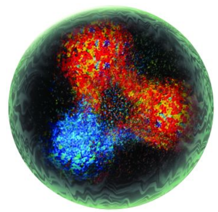

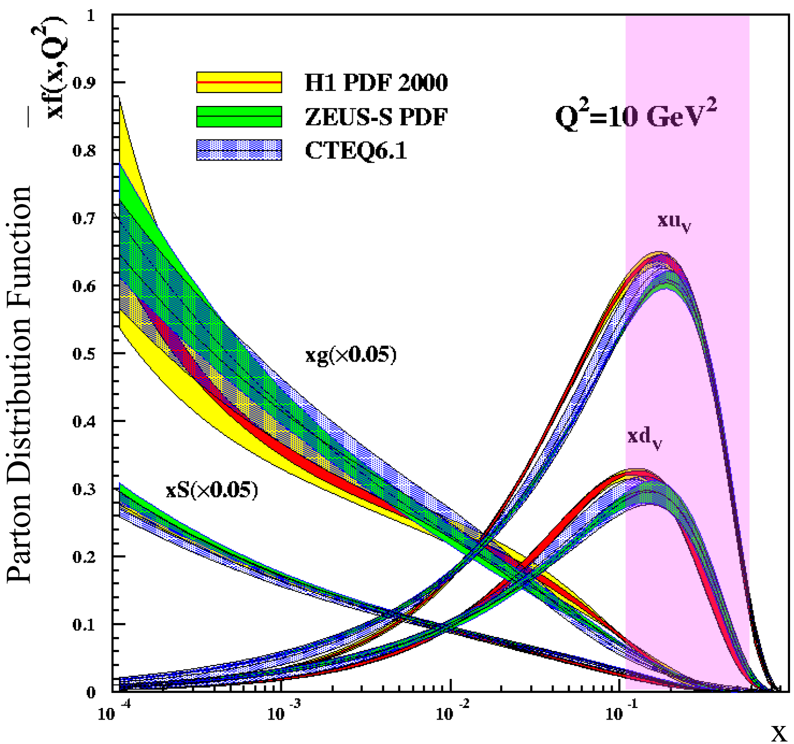

Nucleon at different scales

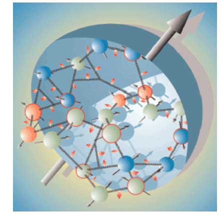

Valence quarks

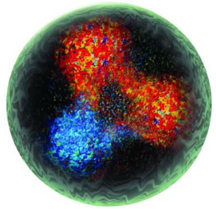

Jefferson Lab: fixed-target electron scattering

$0.1 < x_B < 0.7$

Sea quarks

HERMES: fixed gas-target electron/positron scattering

$0.02 < x_B < 0.3$

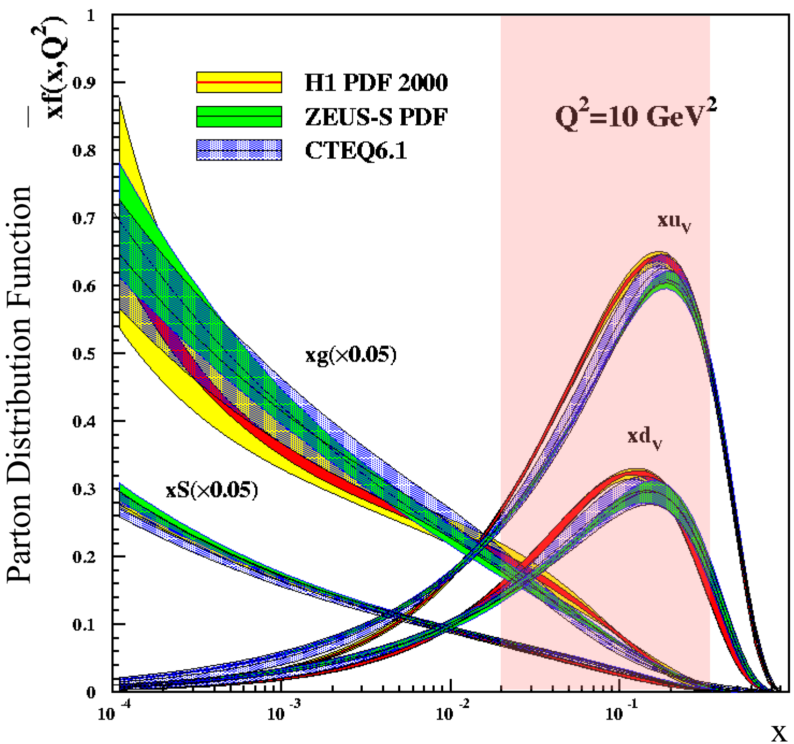

Nucleon at different scales

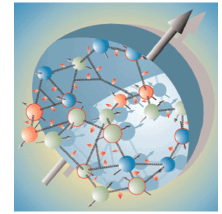

Valence quarks

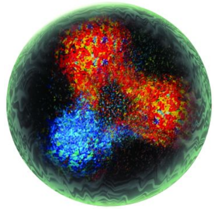

Jefferson Lab: fixed-target electron scattering

$0.1 < x_B < 0.7$

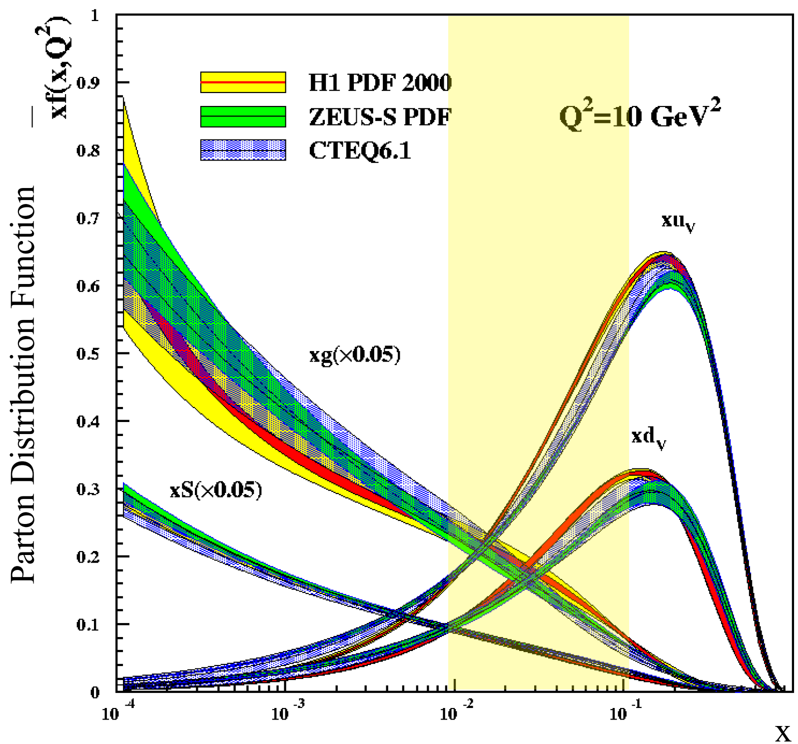

Sea quarks

HERMES: fixed gas-target electron/positron scattering

$0.02 < x_B < 0.3$

COMPASS: fixed-target muon scattering

$0.01 < x_B < 0.1$

Nucleon at different scales

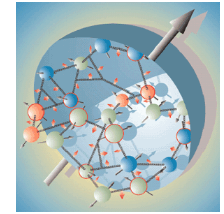

Valence quarks

Jefferson Lab: fixed-target electron scattering

$0.1 < x_B < 0.7$

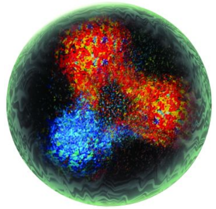

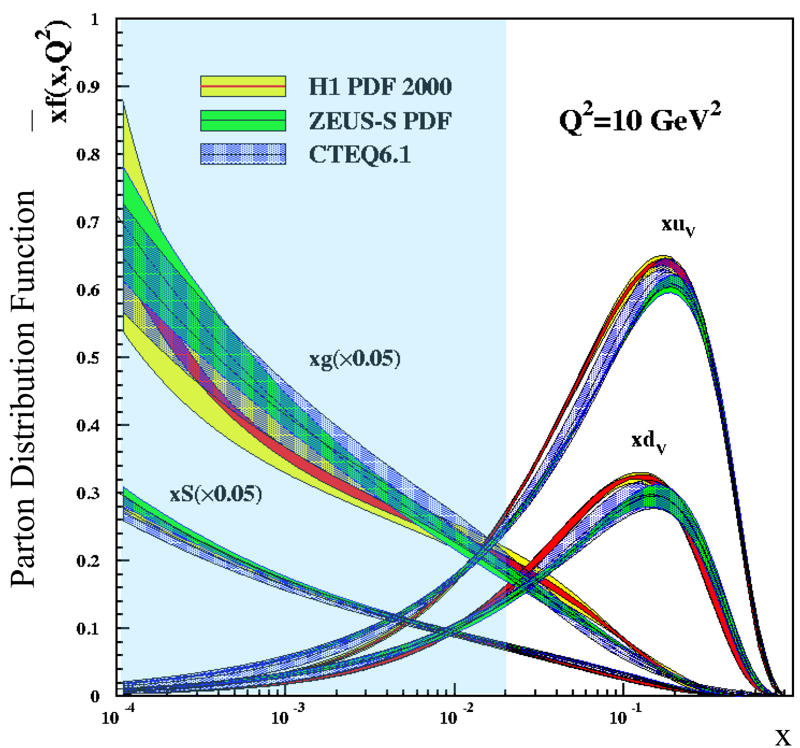

Sea quarks

HERMES: fixed gas-target electron/positron scattering

$0.02 < x_B < 0.3$

COMPASS: fixed-target muon scattering

$0.01 < x_B < 0.1$

The glue

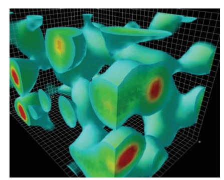

Derek Leinweber

ZEUS/H1: electron/positron-proton collider

$10^{-4} < x_B < 0.02$

Nucleon at different scales

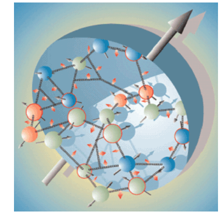

Valence quarks

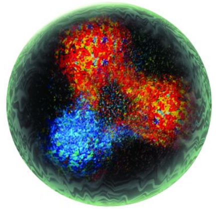

Jefferson Lab: fixed-target electron scattering

$0.1 < x_B < 0.7$

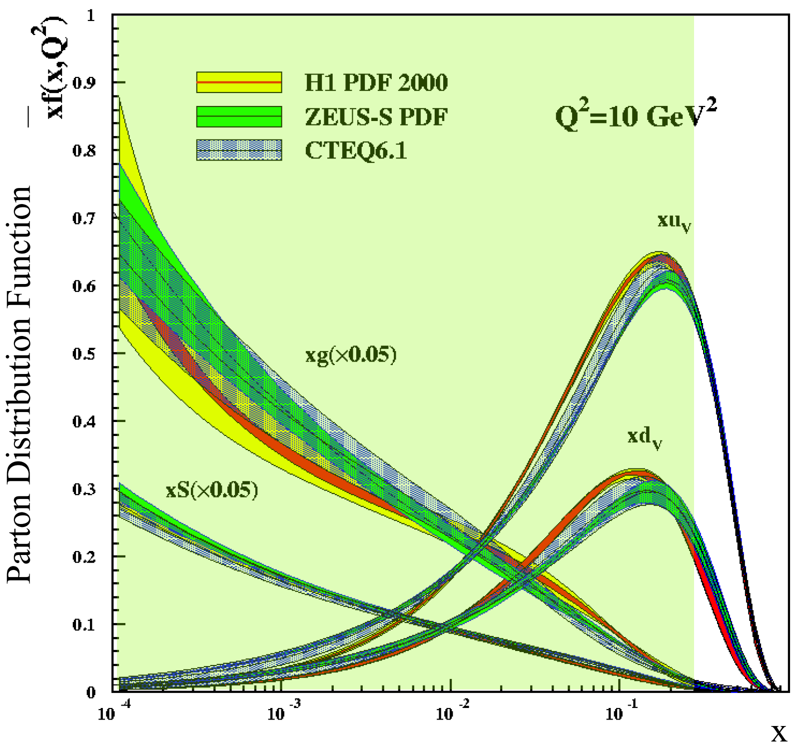

Sea quarks

HERMES: fixed gas-target electron/positron scattering

$0.02 < x_B < 0.3$

COMPASS: fixed-target muon scattering

$0.01 < x_B < 0.1$

The glue

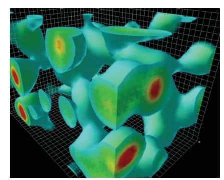

Derek Leinweber

ZEUS/H1: electron/positron-proton collider

$10^{-4} < x_B < 0.02$

Electron-ion collider: $10^{-4} < x_B < 10^{-1}$

Luminosity 100 - 1000 times that of HERA

Jefferson Lab: 6 GeV era

CEBAF: Continuous Electron Beam Accelerator Facility.

- Energy up to ~6 GeV
- Energy resolution $\delta E/E_e \sim 10^{-5}$
- Electron polarisation up to ~85%

Hall A:

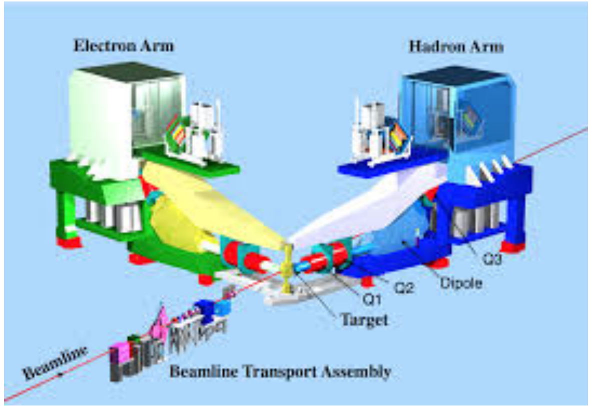

- High resolution($\delta p/p = 10^{-4}$) spectrometers, very high luminosity.

Hall B: CLAS

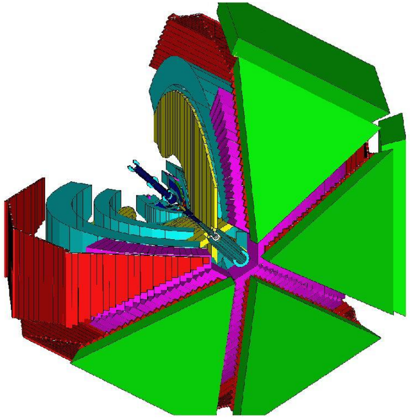

- Very large acceptance, detector array for multi-particle final states.

Hall C:

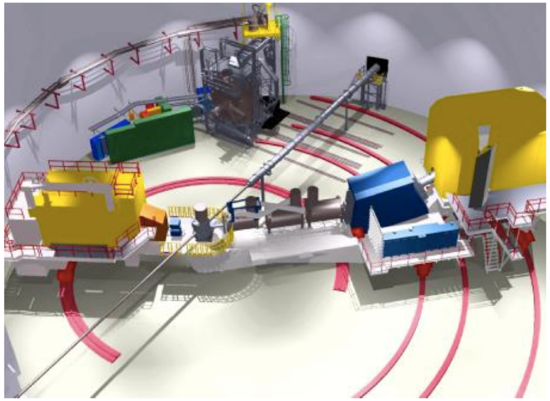

- Two movable spectrometer arms, well-defined acceptance, high luminosity

JLab @ 12 GeV

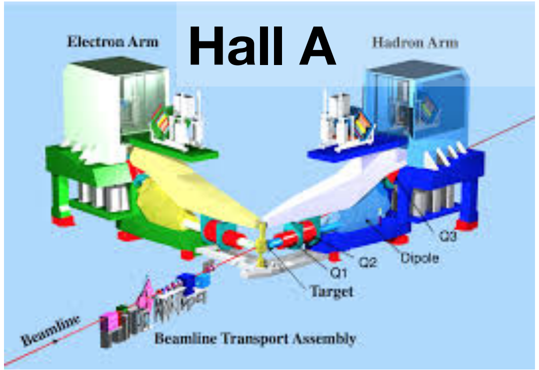

High resolution($\delta p/p = 10^{-4}$) spectrometers, very high luminosity, large installation experiments.

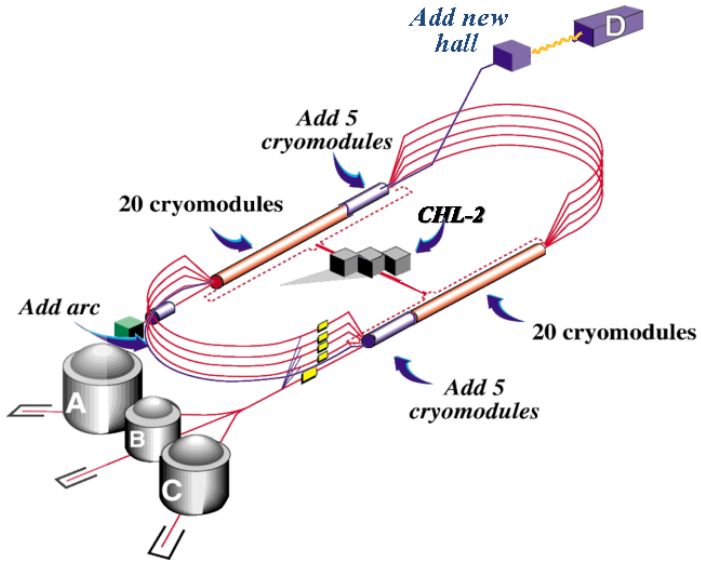

Hall C

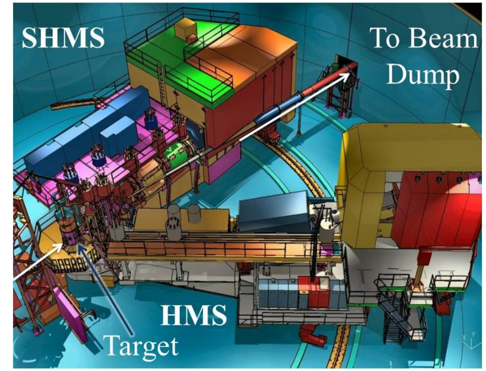

Two movable high momentum spectrometers, well-defined acceptance, very high luminosity.

Hall D

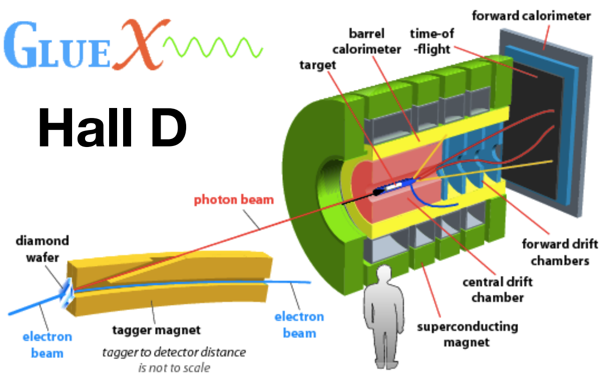

9 GeV tagged polarised photons, full acceptance

Hall B: CLAS12

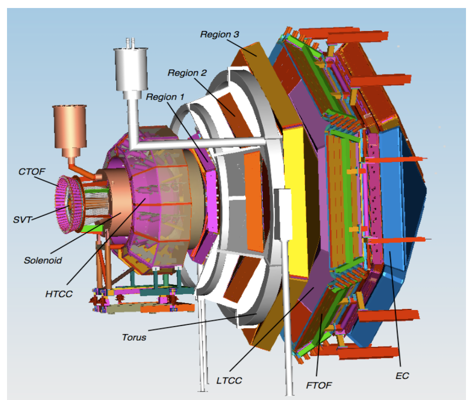

Very large acceptance, high luminosity.

JLab @ 12 GeV

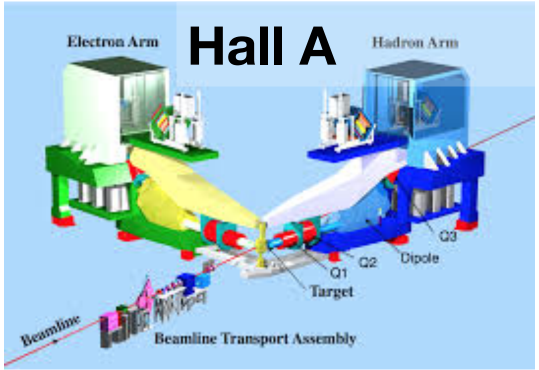

High resolution($\delta p/p = 10^{-4}$) spectrometers, very high luminosity, large installation experiments.

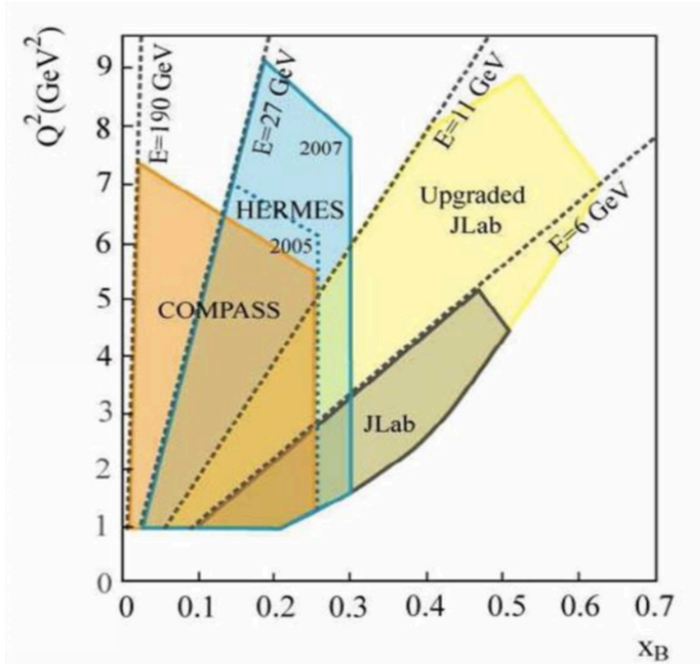

Hall C

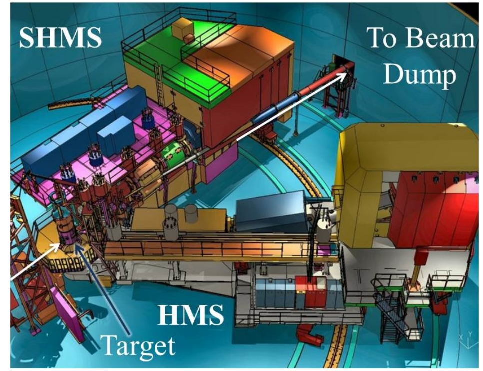

Two movable high momentum spectrometers, well-defined acceptance, very high luminosity.

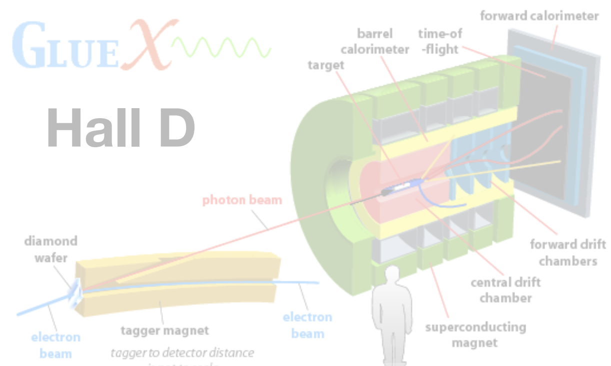

9 GeV tagged polarised photons, full acceptance

Hall B: CLAS12

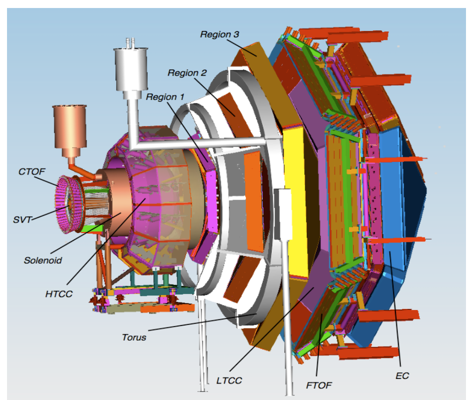

Very large acceptance, high luminosity.

CLAS12

Design luminosity

$L \sim 10^{35}\ cm^{-2}\ s^{-1}$

High luminosity & large acceptance:
Concurrent measurement of exclusive, semi-inclusive, and inclusive processes

Acceptance for photons and electrons:
- $2.5^o < \theta < 125^o$

Acceptance for all charged particles:
- $5^o < \theta < 125^o$

Acceptance for neutrons:
- $5^o < \theta < 120^o$

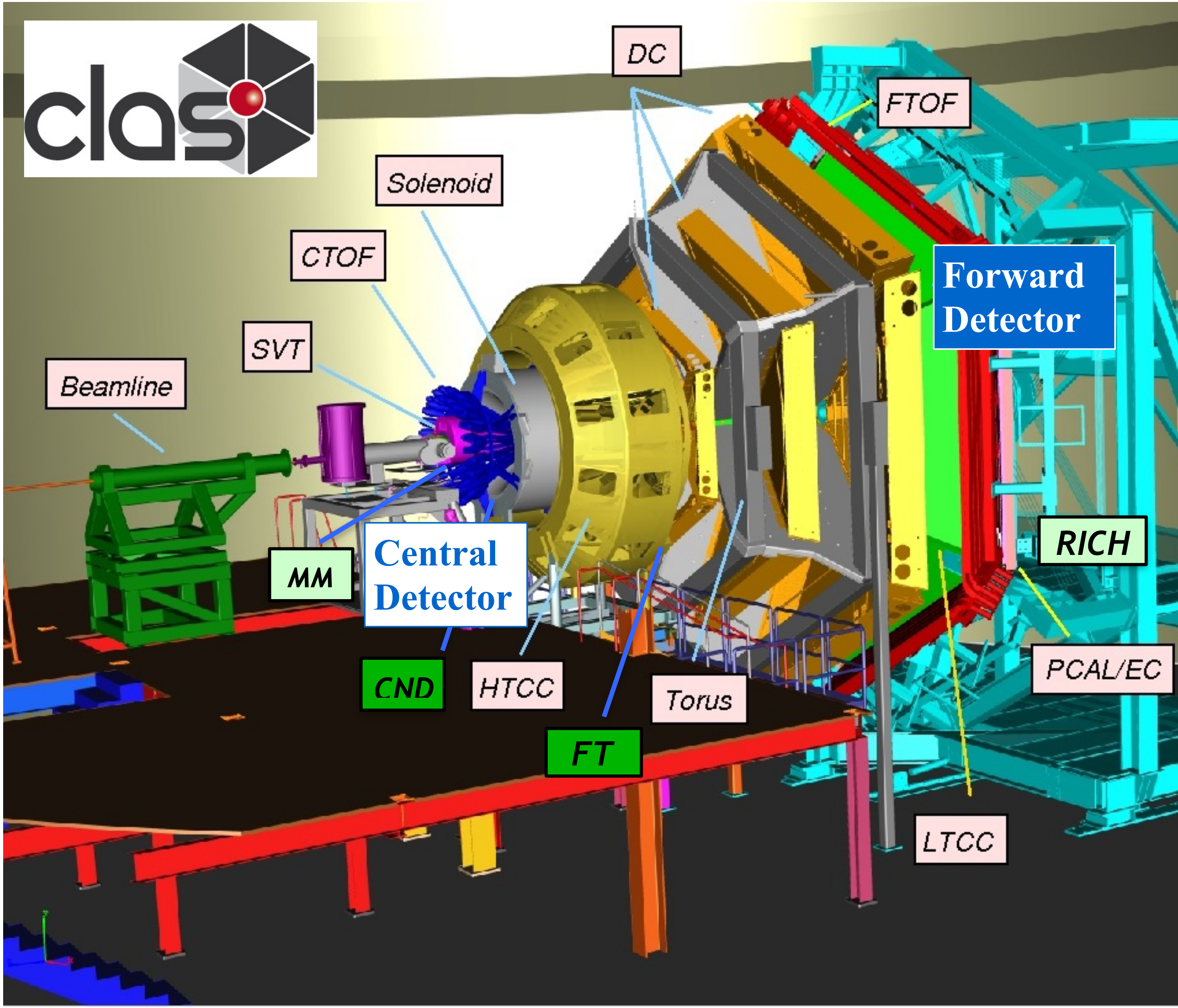

DVCS in Hall C

Detect electron with (Super) High Momentum Spectrometer, (S)HMS.

Detect photon in $PbWO_4$ calorimeter.

Sweeping magnet to reduce backgrounds in calorimeter.

Reconstruct recoiling proton through missing mass.

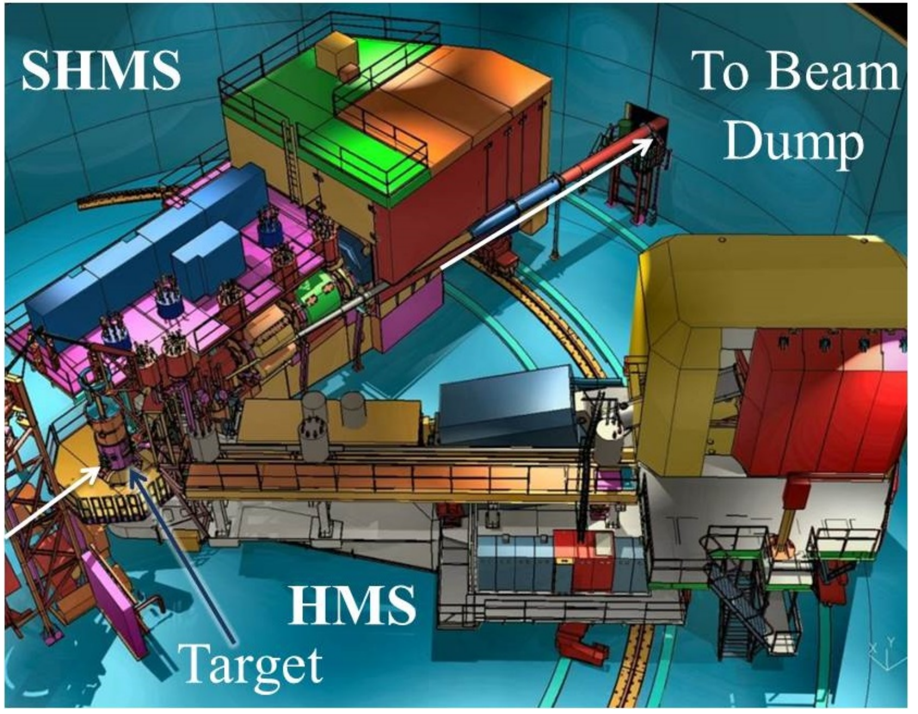

Similar principle applied in Hall A